Investigation of the properties of the QCD-BFKL Pomeron and the Pomeron/Graviton correspondence from HERA data

Motivation for the ep physics at future colliders

Motivation for EIC, see next talk by Vadim Guzey

H. Kowalski,
6th Workshop on High p_T physics at LHC
Utrecht, 6th of April 2011

HERA: the largest e-p collider ever build

Operated between 1992 and 2007

Determination of Gluon Density

GD is determined from the increase of F_2 with x and Q^2 in low-x region

Recent progress, precision of F_2 increased by more than a factor 2

DGLAP describes data very well but deviations are seen when the low Q^2 cut change from 2 to 5 GeV:

χ^2 [818/806 → 698/771]

Today precision of GD O(10) %

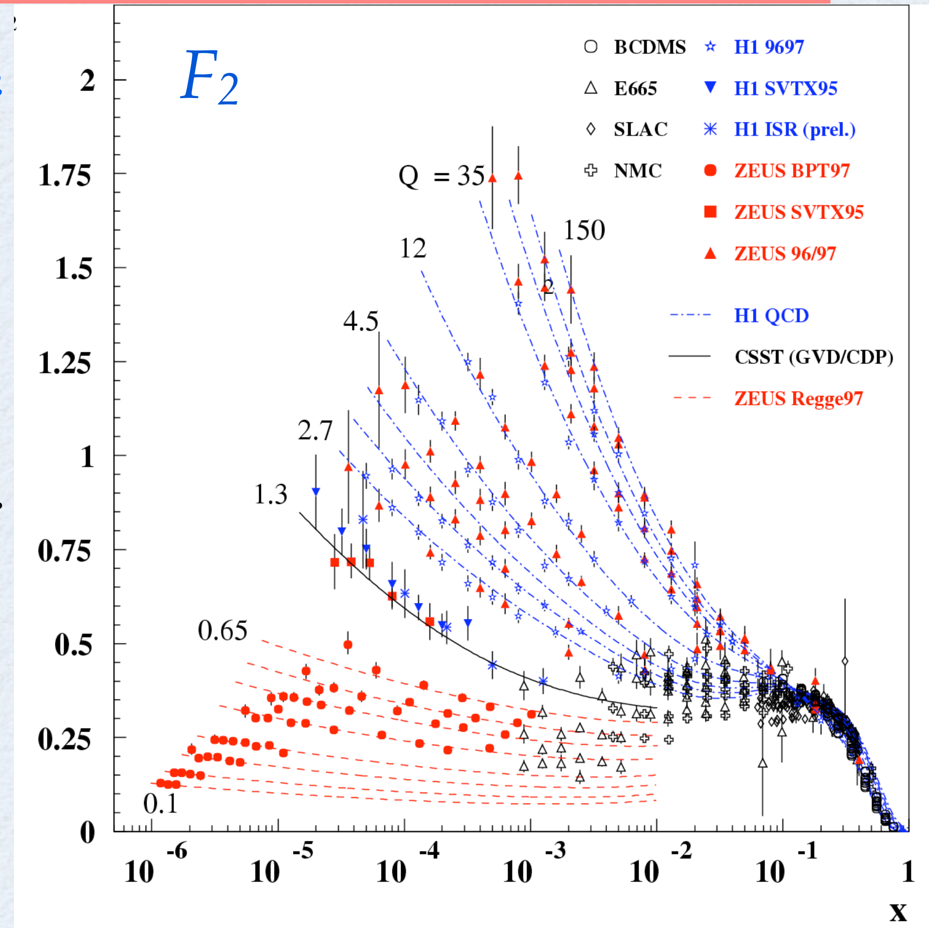

e.g.: valence quark contribution varies by about 5 to 10% in low-x, substantial differences between v.q contributions for MSTW, CTEQ or HERAPDF

another sign of a problem with DGLAP at small x,
negative gluons in addition to higher $\chi 2$ of fits

a solution has to involve
matching of BFKL
or BK equations with DGLAP

matching requires high
precision data

e.g.
recent BFKL analysis of HERA
data by HK, Lipatov, Ross. Watt,
arXiv(1005.0355);

BK analysis by Albacete et al
BFKL+DGLAP,Thorn and
White

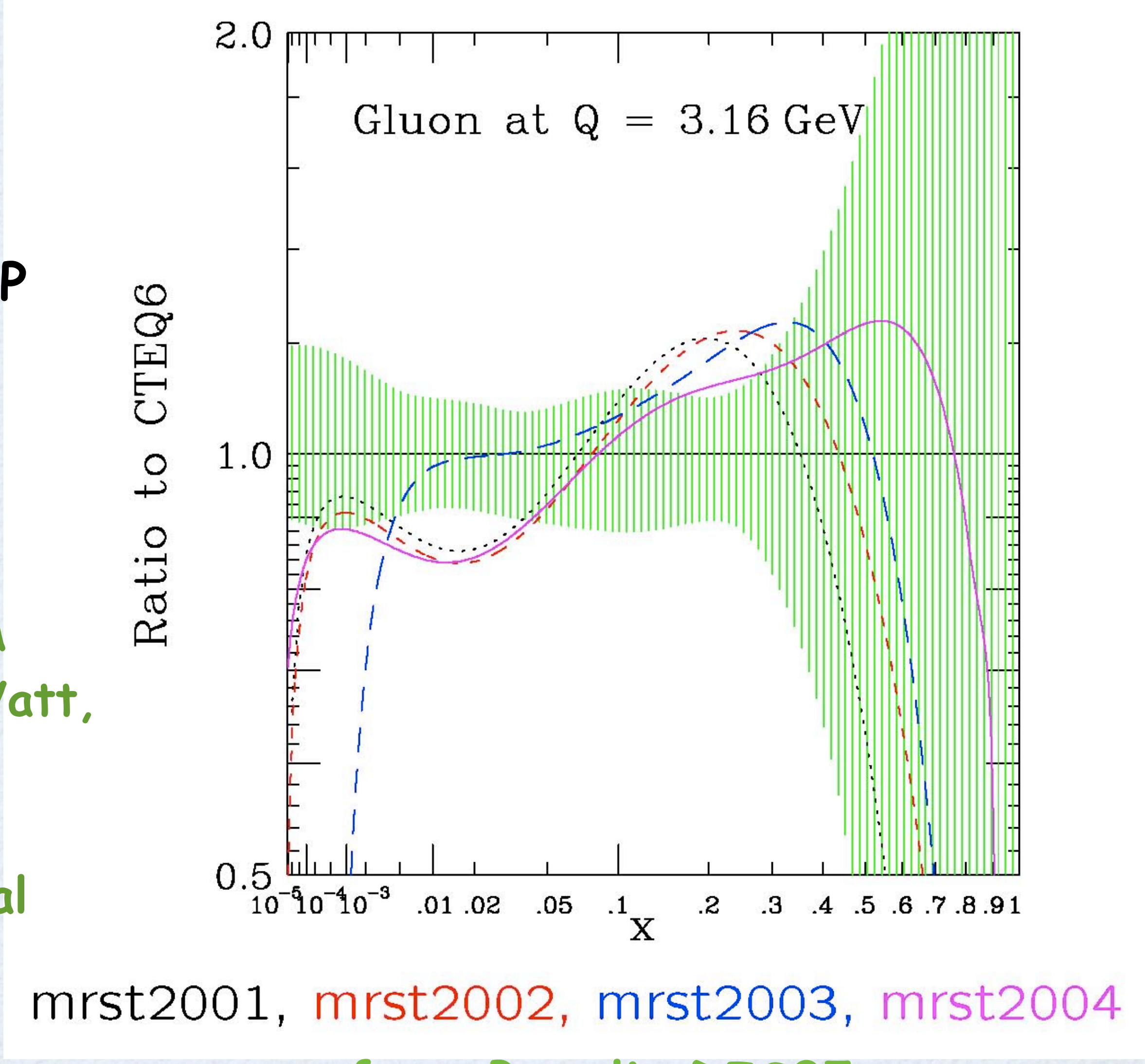

from Pumplin DIS05

Partons vs Dipoles

Infinite momentum frame: Partons

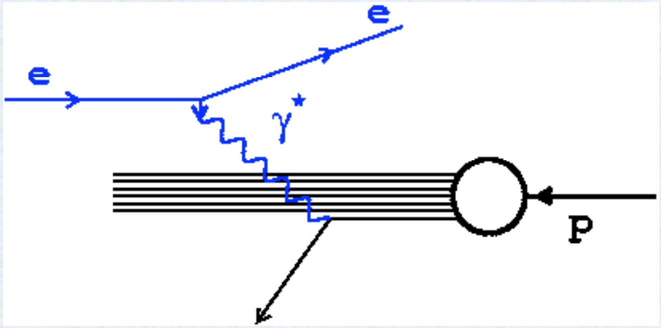

F_2 measures parton density at a scale Q^2

$$F_2 = \Sigma_f \, e_f^2 \, xq(x, Q^2)$$

Proton rest frame: Dipoles - long living quark pair interacts with the gluons of the proton *dipole life time ≈ 1/(m_p x) = 10 - 1000 fm at x = 10^{-2} - 10^{-4}*

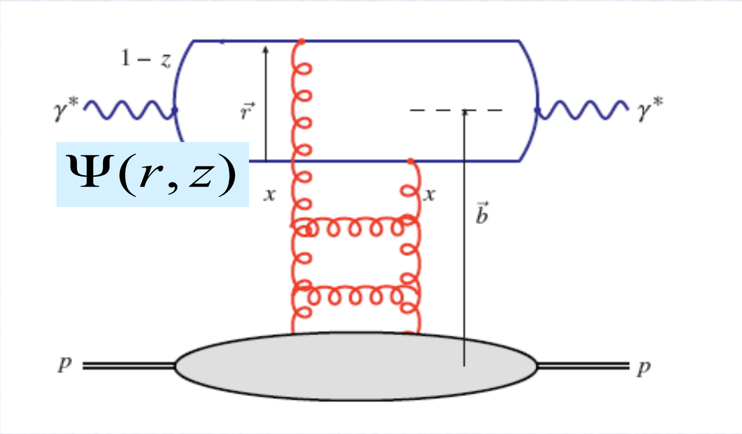

$$\sigma_{tot}^{\gamma^* p} = \int \Psi^* \sigma_{qq} \Psi \; ; \qquad F_2 = \frac{Q^2}{4\pi^2 \alpha_{em}} \sigma_{tot}^{\gamma^* p}$$

for small dipoles, at low-x, dipole picture is equivalent to the QCD parton picture

HERA - F_2 is dominated by the gluon density at low x

➤ **the same gluon density determines the exclusive and inclusive diffractive processes,**

$\gamma p \Rightarrow J/\psi\ p,\ \gamma p \Rightarrow \varphi p,\ \gamma p \Rightarrow \rho p,\quad \gamma p \Rightarrow Xp,$

➤ **universal gluon density ≡ Pomeron ?**

F_2

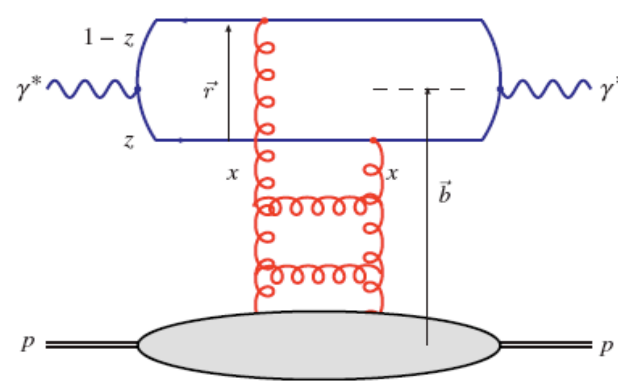

VM, Diffraction

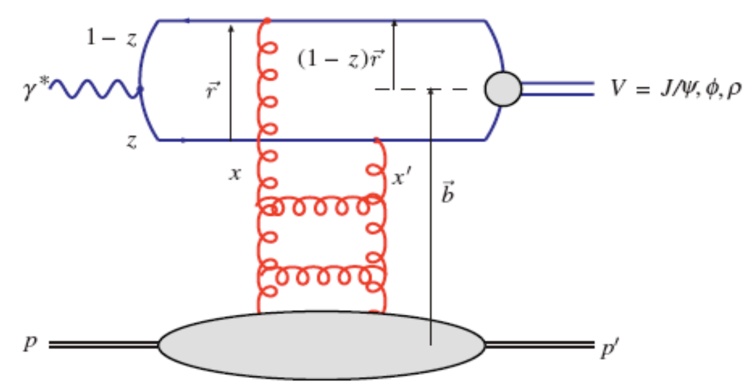

clear hints for saturation, but here we concentrate on the gluon gluon interactions above the saturation region

Vector Mesons

KMW
PRD 74 074016
PRD 78 014016

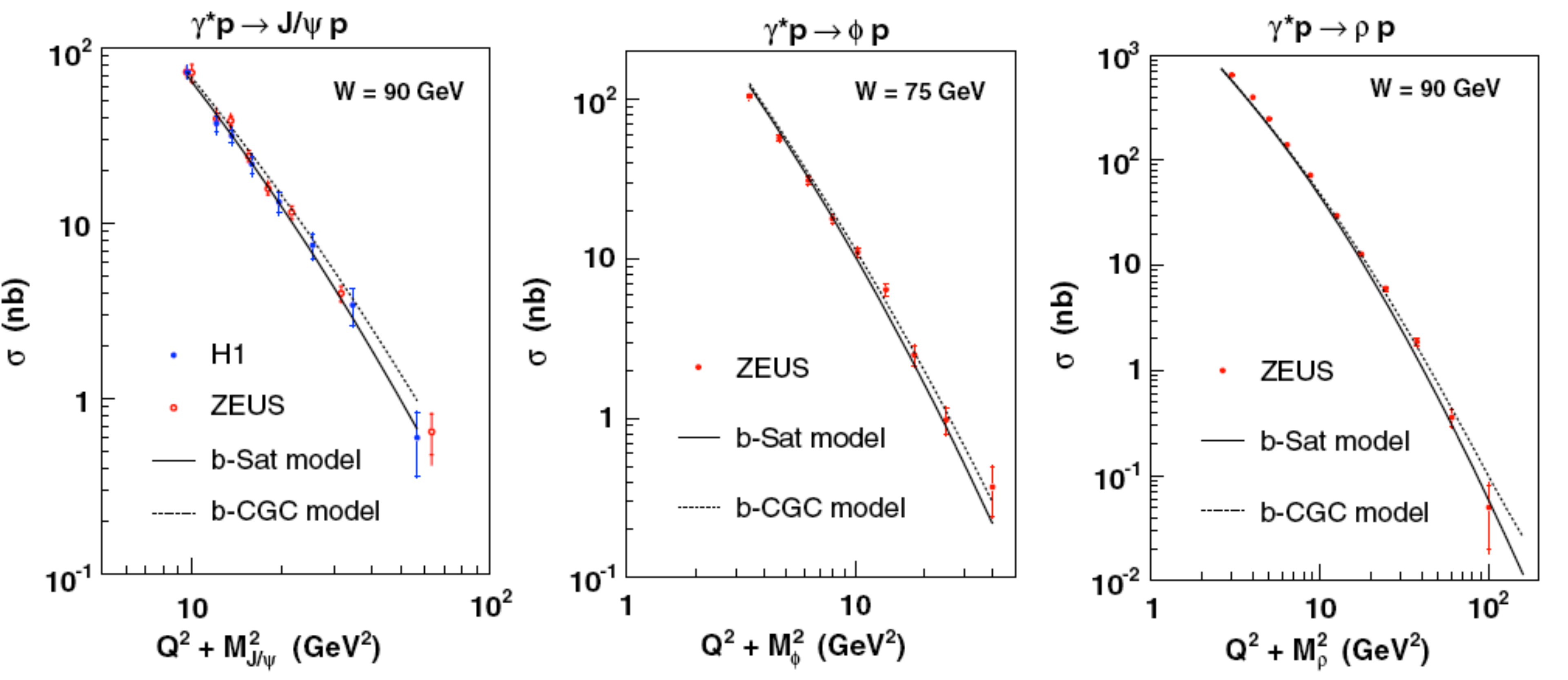

Note: educated guesses for VM wf are working very well

In focus: Exclusive J/psi production

educated guess for VM wf is working very well for J/psi and phi and DVCS

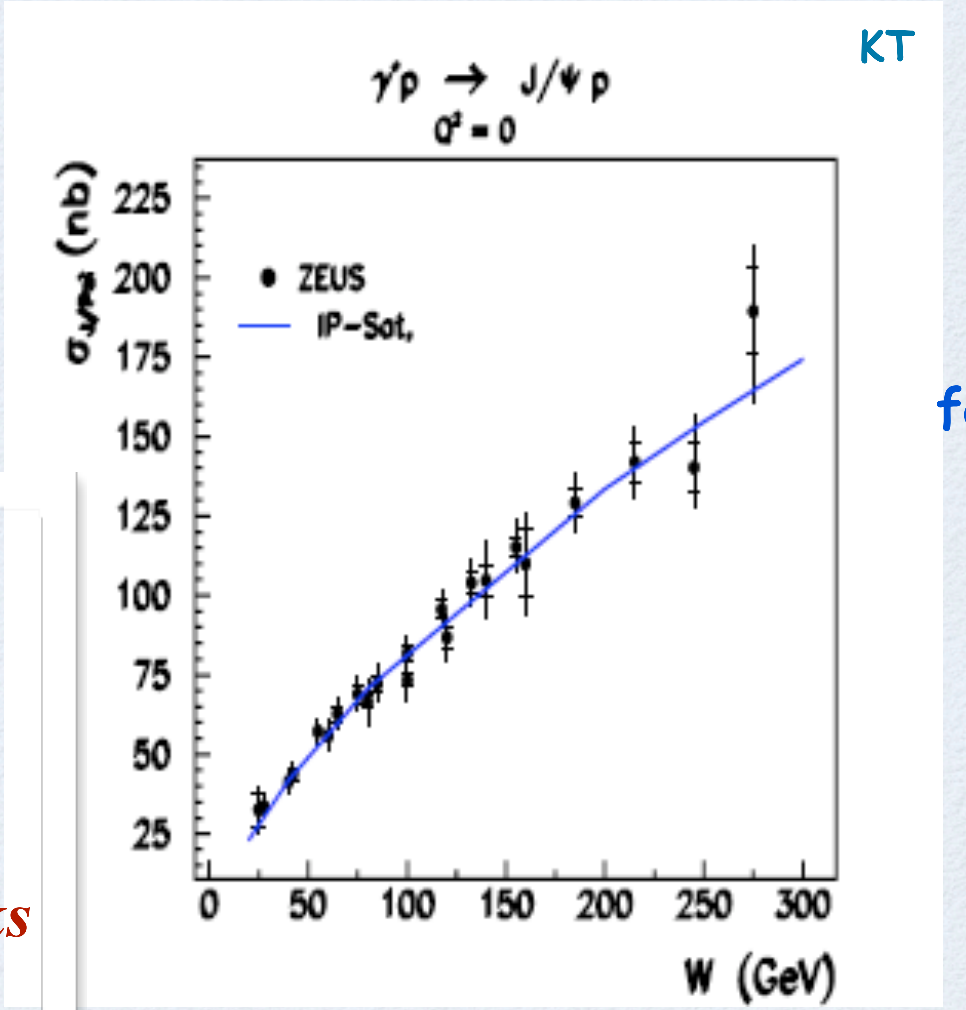

equally good description of Q2 and σ_L/σ_T dependences for J/psi and phi and DVCS

Note:
J/psi x-section grows almost like
$\sigma \propto (x\, g(x,\mu^2))^2$
no valence quarks contribution

➤ **the determination of gluon density with J/psi would be more precise than by F_2 or F_L (MRT) if J/psi would have small systematic errors**

Extracting Proton Shape using dipoles

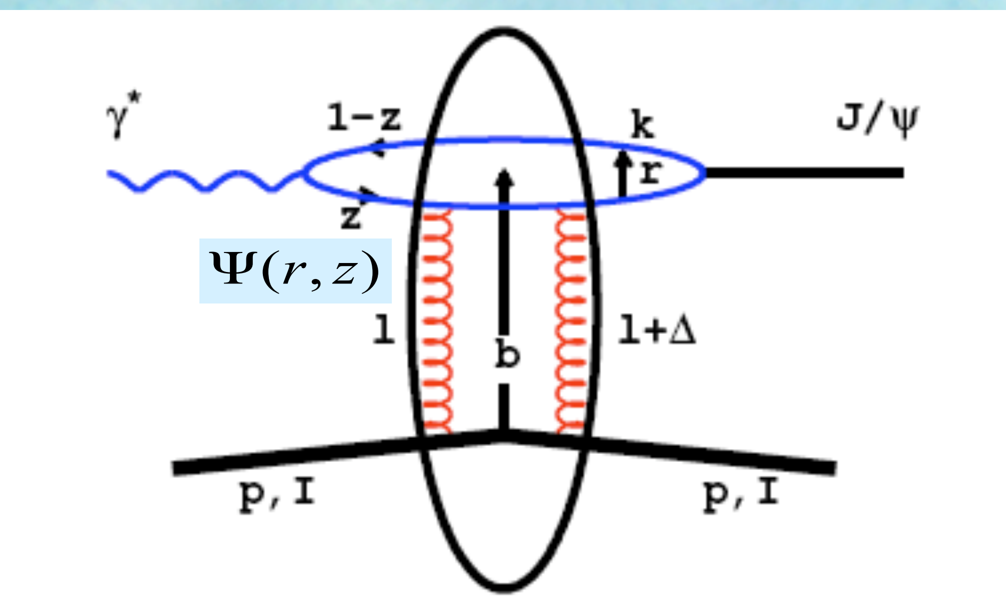

$\Psi(r,z)$

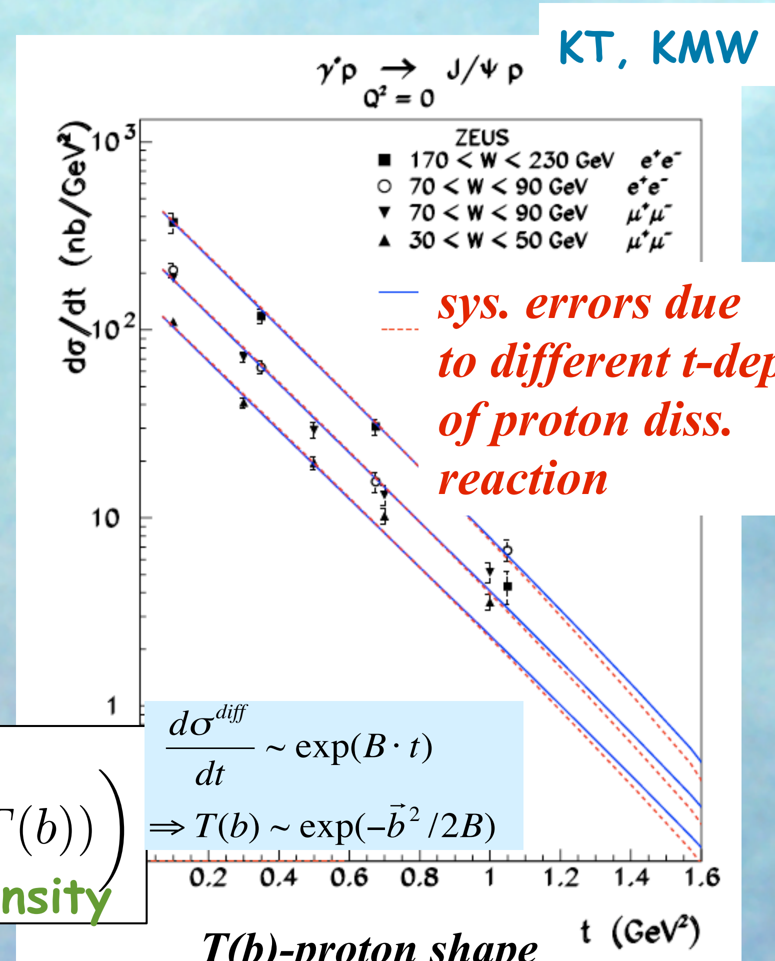

sys. errors due to different t-dep. of proton diss. reaction

$$\frac{d\sigma^{diff}}{dt} \sim \exp(B \cdot t)$$

$$\Rightarrow T(b) \sim \exp(-\vec{b}^2/2B)$$

T(b)-proton shape

$$\frac{d\sigma_{qq}}{d^2b} = 2\left(1 - \exp(-\frac{\pi^2}{2N_C} r^2 \alpha_s(\mu^2)\, xg(x,\mu^2)\, T(b))\right)$$

for larger gluon density

v.g. description of B for all VM and DVCS with the same wf ansatz
➡ determination of the gluonic proton radius, r_{gg} = 0.6 fm is smaller than the quark radius r_p=0.9 fm

Why to investigate Gluon Density?

- it determines important physics reactions, like Higgs or gluonic di-jet production, at LHC

- Gluon Density ≡ Pomeron determines the high energy behavior of scattering amplitudes

  high energy behavior of scattering amplitudes is connected to the long range behavior of nuclear forces ⇒ confinement

- it is a fundamental physics quantity

The dynamics of Gluon Density at low x is determined by **the amplitude for the scattering of a gluon on a gluon**, described by the BFKL equation

$$\frac{\partial}{\partial \ln s}\mathcal{A}(s,\mathbf{k},\mathbf{k}') = \delta(k^2 - k'^2) + \int dq^2 \mathcal{K}(\mathbf{k},\mathbf{q})\mathcal{A}(s,\mathbf{q},\mathbf{k}')$$

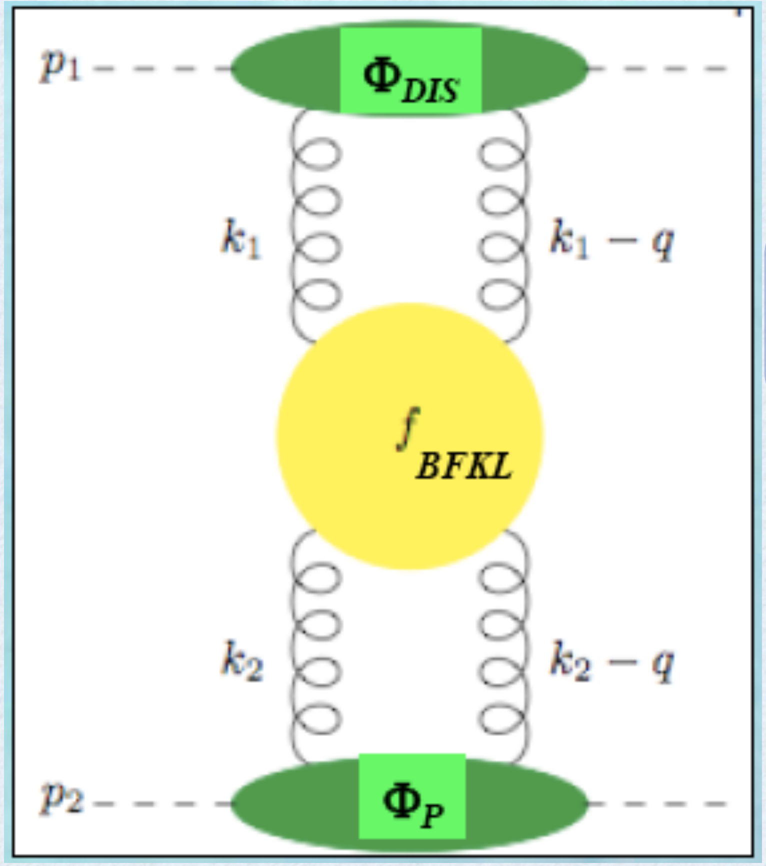

which can be solved in terms of the eigenfunctions of the kernel

$$\int dk'^2 \mathcal{K}(\mathbf{k},\mathbf{k}') f_\omega(\mathbf{k}') = \omega f_\omega(\mathbf{k})$$

in LO, with fixed α_s

$$f_\omega(\mathbf{k}) = \left(k^2\right)^{i\nu - 1/2}$$
$$\omega = \alpha_s \chi_0(\nu)$$

prevailing intuition (based on DGLAP) - gluon are a gas of particles

BFKL leads to a richer structure - basic feature: oscillations

Properties of the BFKL Kernel

Quasi-locality

$$\mathcal{K}(\mathbf{k},\mathbf{k}') = \frac{1}{kk'}\sum_{n=0}^{\infty} c_n \delta^{(n)}\left(\ln(\mathbf{k}^2/\mathbf{k}'^{\,2})\right)$$

$$c_n = \int_0^\infty dk'^{\,2}\mathcal{K}(\mathbf{k},\mathbf{k}')\frac{k}{k'}\frac{1}{n!}\left(\ln(\mathbf{k}^2/\mathbf{k}'^{\,2})\right)^n$$

Similarity to the Schroedinger equation

$$k\int dk'^{\,2}\mathcal{K}(\mathbf{k},\mathbf{k}')f_\omega(\mathbf{k}') = \sum_{n=0}^{\infty} c_n \left(\frac{d}{d\ln(\mathbf{k}^2)}\right)^n \bar{f}_\omega(\mathbf{k}) = \omega\bar{f}_\omega(\mathbf{k})$$

Characteristic function

$$k\int dk'^{\,2}\mathcal{K}(\mathbf{k},\mathbf{k}')f_\omega(\mathbf{k}') = \chi\left(-i\frac{d}{d\ln k^2}, \alpha_s(k^2)\right)\bar{f}_\omega(k) = \omega\bar{f}_\omega(k)$$

BFKL amplitude

$$A(s,\mathbf{k_1},\mathbf{k_2}) \sim \int d\nu \left[\frac{\mathbf{k_1^2}}{\mathbf{k_2^2}}\right]^{i\nu} s^{\bar{\alpha}_\mathrm{s}\chi(\nu)}$$

$$\bar{\alpha}_s = C_A \frac{\alpha_s}{\pi}$$

Diffusion approximation

$$\chi(\nu) = 4\ln(2) - 7\zeta(3)\nu^2 + \ldots$$

$$\mathcal{A}(s,t,\mathbf{k_1},\mathbf{k_2}) \sim \int d\nu\, s^{1+\overline{\alpha_s}\left(4\ln(2)-7\zeta(3)\nu^2+\cdots\right)} e^{i\nu(ln(\mathbf{k_2})-ln(\mathbf{k_1}))}$$

BFKL eq., with fixed α_s, predicts $F_2 \sim (1/x)^{\omega}$ with $\omega \sim$ constant with Q^2, $\omega \sim 0.5$ in LO and $\omega \sim 0.3$ in NLO

Therefore, the prevailing opinion was that the BFKL analysis is not applicable to HERA data.

The rate of rise λ

$F_2 \sim (1/x)^{\lambda}$

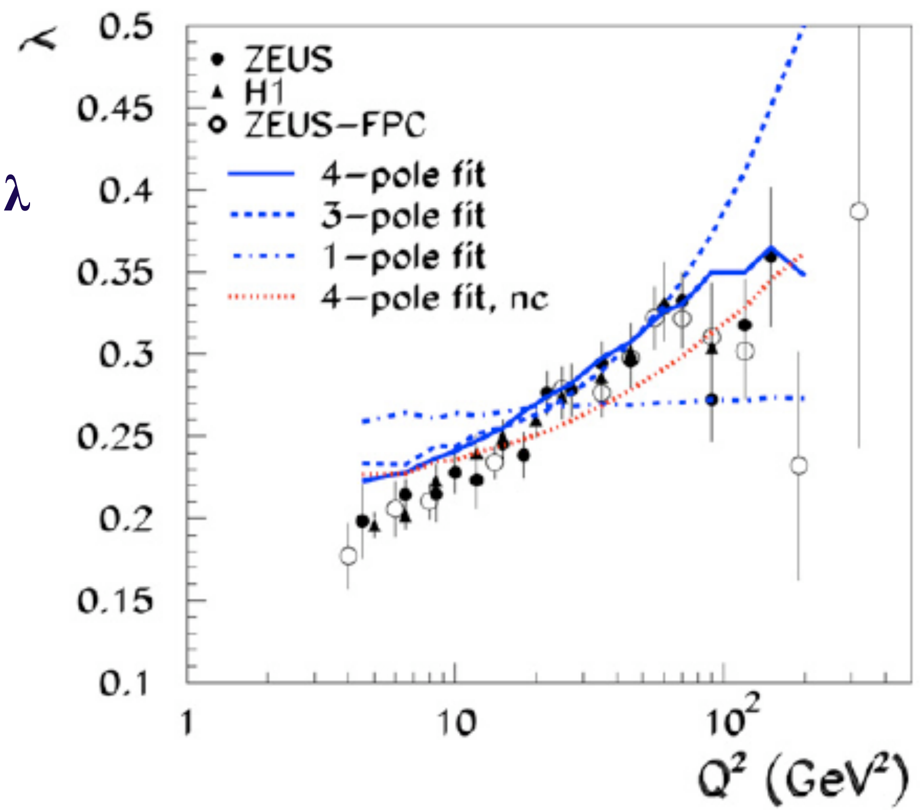

First hints that in BFKL λ can be substantially varying with Q^2 was given in PL 668 (2008) 51 by EKR

Lipatov 86 & EKR 2008: BFKL solutions with the running α_s are substantially different from solutions with the fixed α_s.

in NLO, with running α_s, BFKL frequency ν becomes k-dependent, $\nu(k)$

$$\alpha_s(k^2)\chi_0(\nu(\mathbf{k})) + \alpha_s^2(k^2)\chi_1(\nu(\mathbf{k})) \ = \ \omega$$

ν has to become a function of k because ω cannot depend on k

GS resummation applied

evaluation in diffusion ($\nu \approx 0$) or semiclassical approximation ($\nu > 0$)

For sufficiently large k, there is no longer a real solution for ν.

The transition from real to imaginary $\nu(k)$ singles out a special value of

$k = k_{crit}$, with $\nu(k_{crit}) = 0$.

The solutions below and above this critical momentum k_{crit} have to match. This fixes the phase of ef's.

Near $k = k_{crit}$, the BFKL eq. becomes the Airy eq. which is solved by the Airy eigenfunctions

$$k\, f_\omega(k) = \bar{f}_\omega(k) = \mathrm{Ai}\left(-(\frac{3}{2}\phi_\omega(k))^{\frac{2}{3}}\right)$$

with

$$\phi_\omega(k) = 2\int_k^{k_{\mathrm{crit}}} \frac{d\,k'}{k'} |\nu_\omega(k')|$$

for $k << k_{crit}$ the Airy function has the asymptotic behaviour

$$k\, f_\omega(k) \sim \sin\left(\phi_\omega(k) + \frac{\pi}{4}\right)$$

The two fixed phases at $k = k_{crit}$ and at $k = k_0$ (near Λ_{QCD}) lead to the quantization condition

$$\phi_\omega(k_0) = \left(n - \frac{1}{4}\right)\pi + \eta\,\pi$$

The first eight eigenfunctions determined at η=0

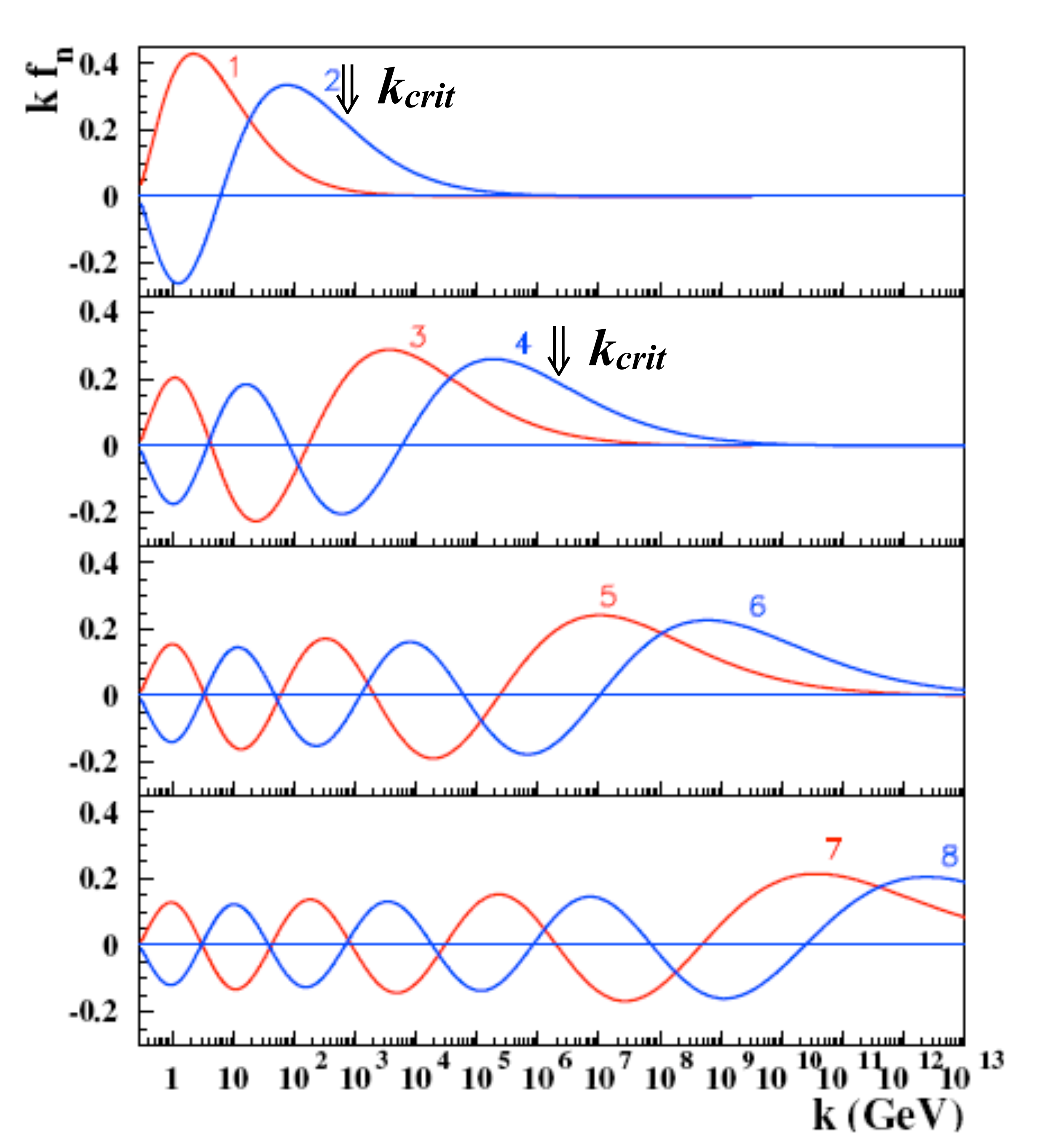

Comparison with HERA data

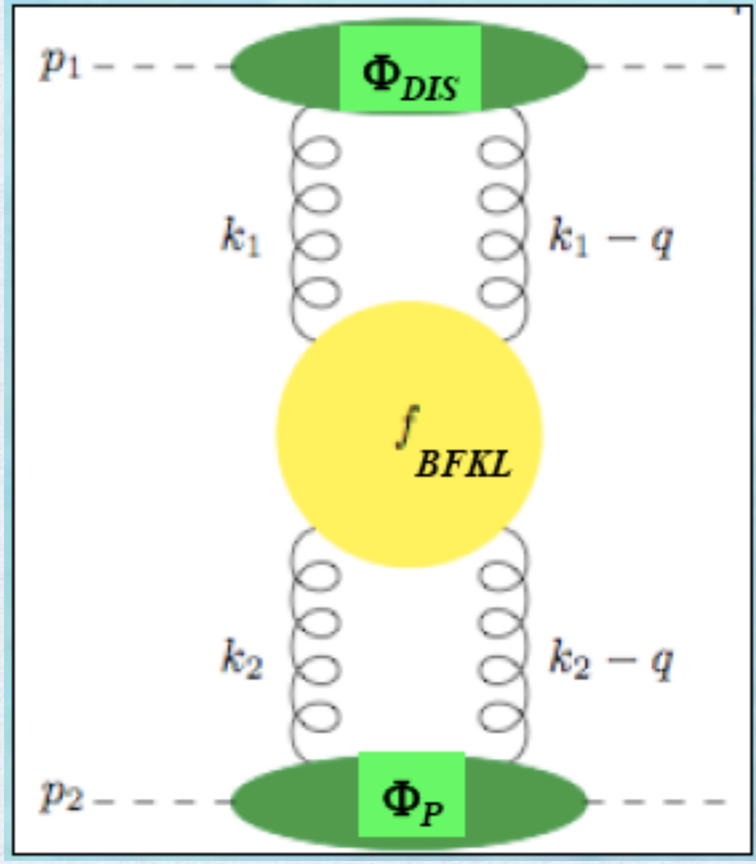

Discreet Pomeron Green function

$$\mathcal{A}(\mathbf{k}, \mathbf{k}') = \sum_{m,n} f_m(\mathbf{k}) \mathcal{N}^{-1}_{mn} f_n(\mathbf{k}') \left(\frac{s}{kk'} \right)^{\omega_n}.$$

Integrate with the photon and proton impact factors

$$\mathcal{A}^{(U)}_n \equiv \int_x^1 \frac{d\xi}{\xi} \int \frac{dk}{k} \Phi_{\mathrm{DIS}}(Q^2, k, \xi) \left(\frac{\xi k}{x} \right)^{\omega_n} f_n(\mathbf{k})$$

$$\mathcal{A}^{(D)}_m \equiv \int \frac{dk'}{k'} \Phi_p(k') \left(\frac{1}{k'} \right)^{\omega_m} f_m(\mathbf{k}').$$

$$F_2(x, Q^2) = \sum_{m,n} \mathcal{A}^{(U)}_n \mathcal{N}^{-1}_{nm} \mathcal{A}^{(D)}_m$$

Proton impact factor

$$\Phi_p(\mathbf{k}) \;=\; A\,k^2 e^{-bk^2}$$

The fit is not sensitive to the particular form of the impact factor.

The support of the proton impact factor is much smaller than the oscillation period of f_n and because the frequencies ν have a limited range

- **many eigenfunctions have to contribute and η has to be a function of n**

$$\eta \;= \eta_0 \left(\frac{n-1}{n_{\max}-1} \right)^{\kappa}$$

The frequencies $\nu(k)$

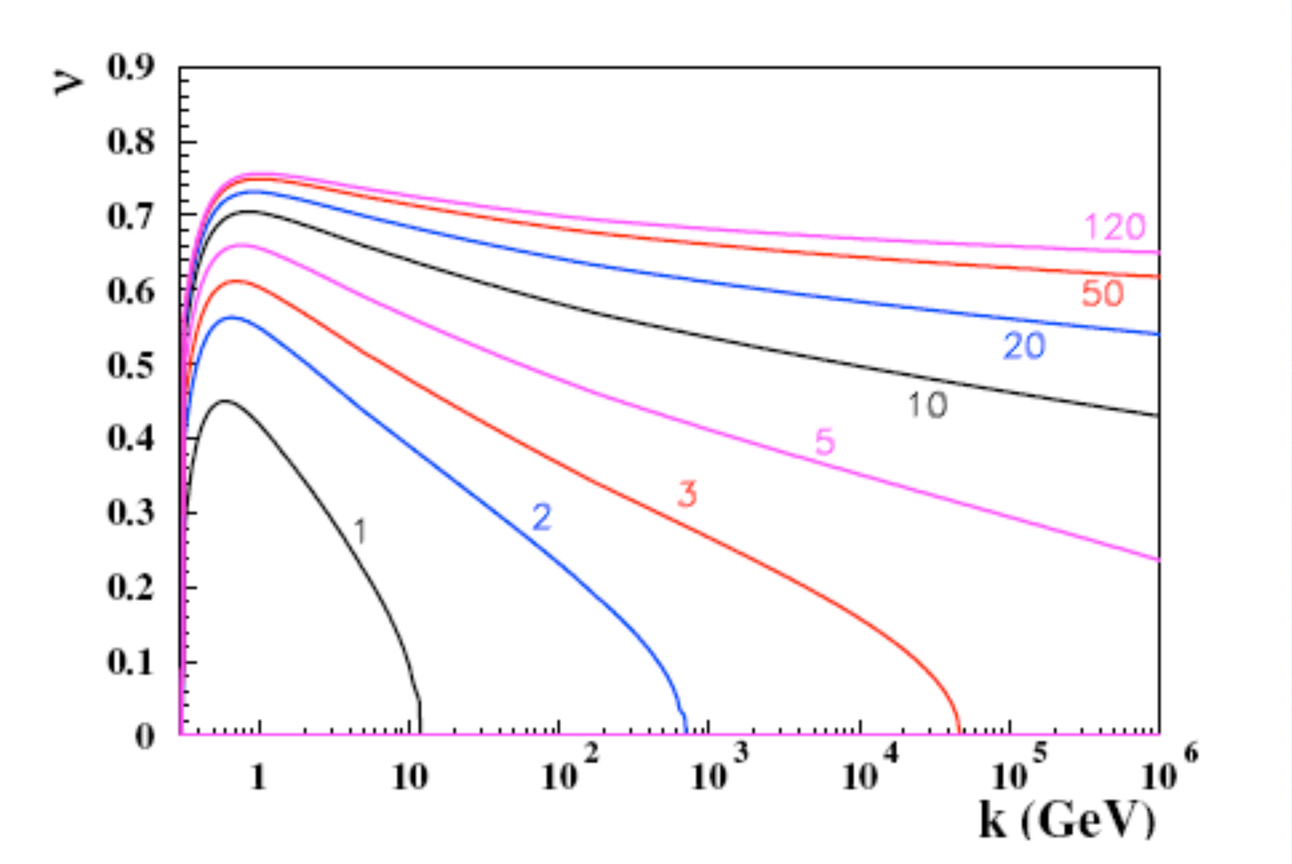

Music analogy:
eigenfunctions are tones with modulated frequencies

The qualities of fits for various numbers of eigenfunctions

(a) Fits with cuts of $Q^2 > 4\ \mathrm{GeV}^2$ and $x < 0.01$

$n_{\max}$	$\chi^2/N_{\mathrm{df}}(x<0.01)$	$\chi^2/N_{\mathrm{dat}}(x<0.001)$	κ	A	b
1	$9792/125=78.3$	$2123/43=49.4$	–	156	30.0
5	$349.8/125=2.80$	$88.8/43=2.07$	3.78	$3.1\cdot10^6$	78.0
20	$286.5/125=2.29$	$83.3/43=1.94$	0.96	632	15.8
40	$193.3/125=1.55$	$54.9/43=1.28$	0.84	2315	23.2
60	$163.3/125=1.31$	$44.8/43=1.04$	0.78	3647	25.6
80	$156.5/125=1.25$	$43.5/43=1.01$	0.73	3081	24.4
100	$149.1/125=1.19$	$41.3/43=0.96$	0.69	2414	22.8
120	$143.7/125=1.15$	$39.2/43=0.91$	0.66	2041	21.8

➤ new data are crucial for finding the right solution

the differences in the fit qualities would be negligible if the errors where more than 2-times larger

The final fit performed with 120 ef's and 30 overlaps and 5 flavours

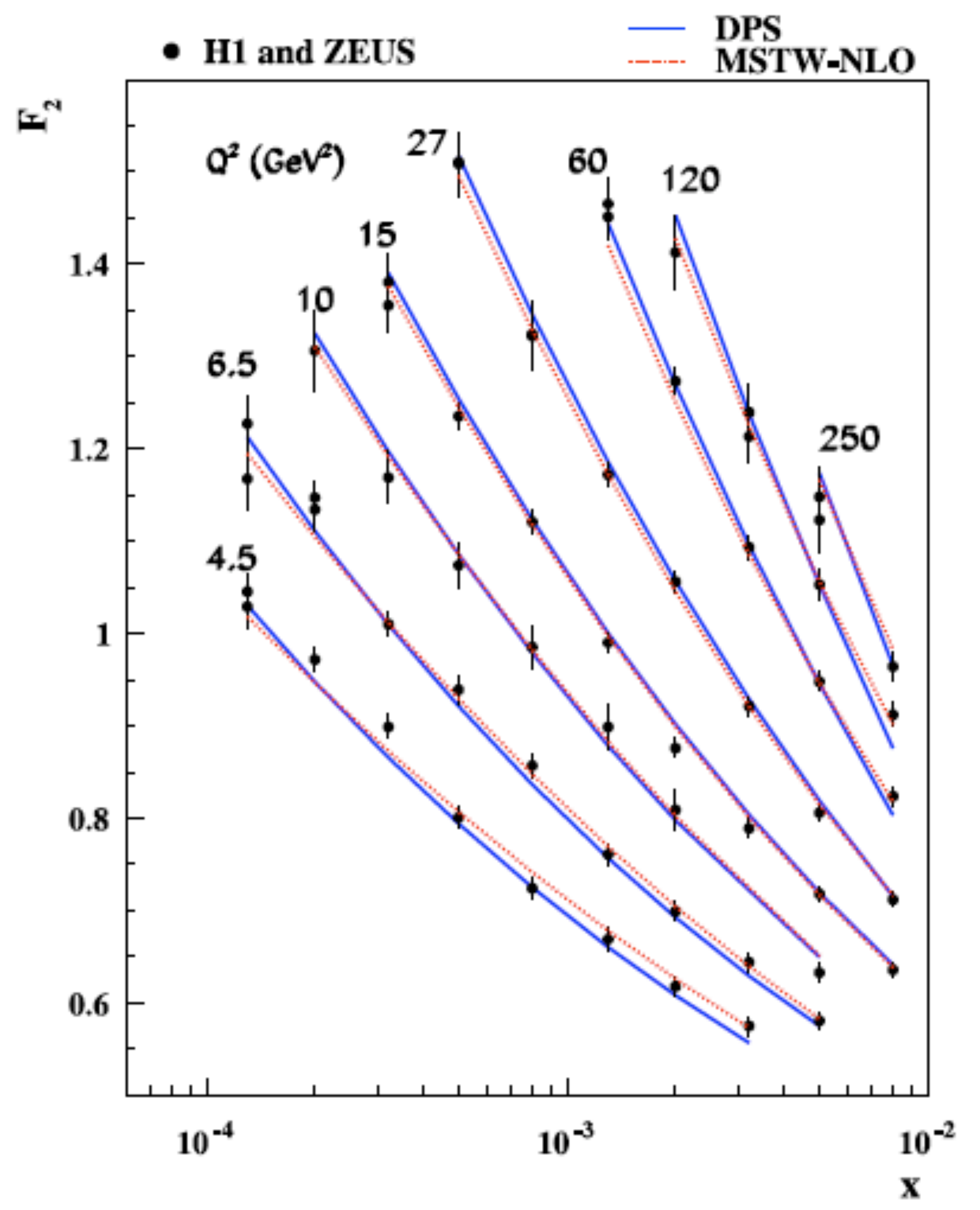

χ^2/N_{df}	κ	A	b
154.7 / 125	0.65	1660	20.6

The rate of rise λ

$F_2 \sim (1/x)^{\lambda}$

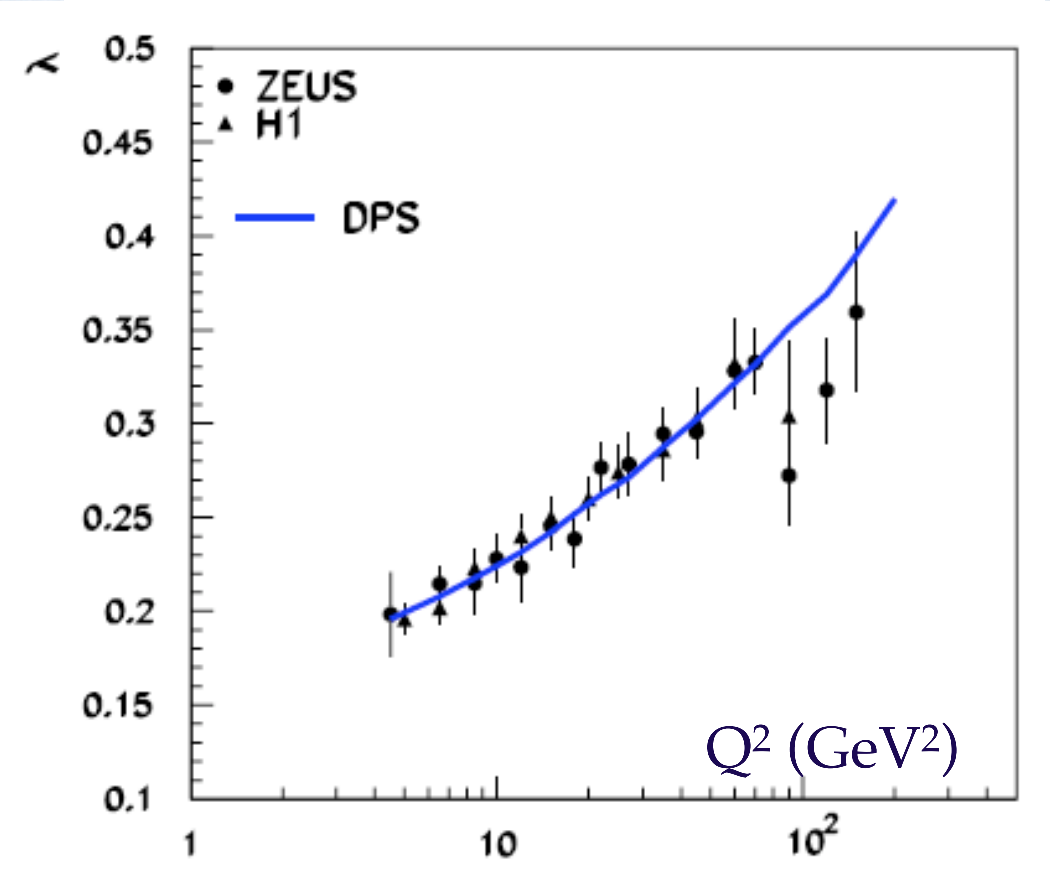

The first successful pure BFKL description of the λ plot.

For many years it was claimed that BFKL analysis was not applicable to HERA data because of the observed substantial variation of λ with Q^2

Eigenvalues ω

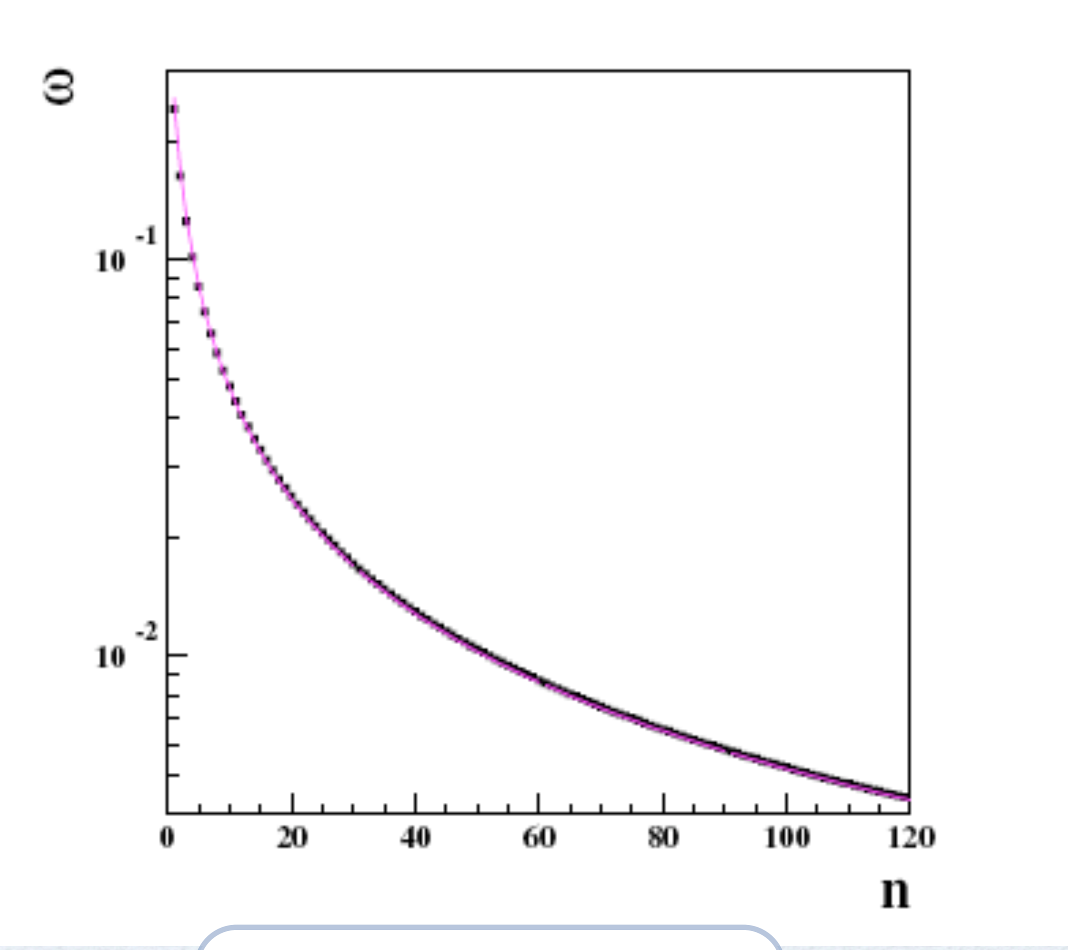

$$\omega_n \approx \frac{0.5}{1 + 0.95\,n}$$

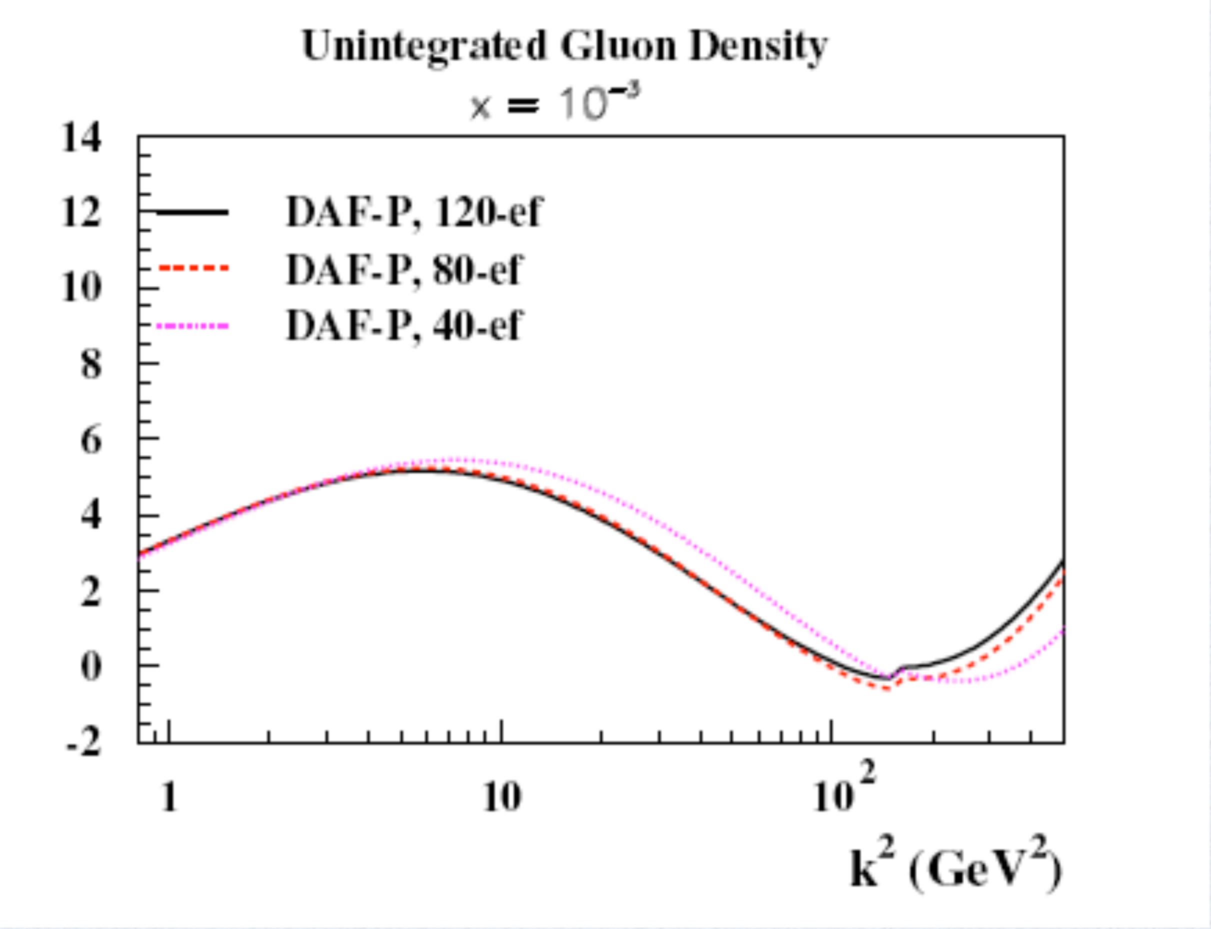

Unintegrated Gluon Density
x = 10^-3
DAF-P, 120-ef
DAF-P, 80-ef
DAF-P, 40-ef
14
12
10
8
6
4
2
0
-2
1
10
10^2
k^2 (GeV^2)

why so many eigenfunctions ?

because the contribution of large n ef's is only weakly suppressed

enhancement by $(1/x)^{\omega}$ is not very large because

$\omega_1 \approx 0.25, \quad \omega_5 \approx 0.1, \quad \omega_{10} \approx 0.05$

suppression of large n contribution only by the normalization condition $\sim 1/\sqrt{n}$

The first eight eigenfunctions determined at $\eta=0$

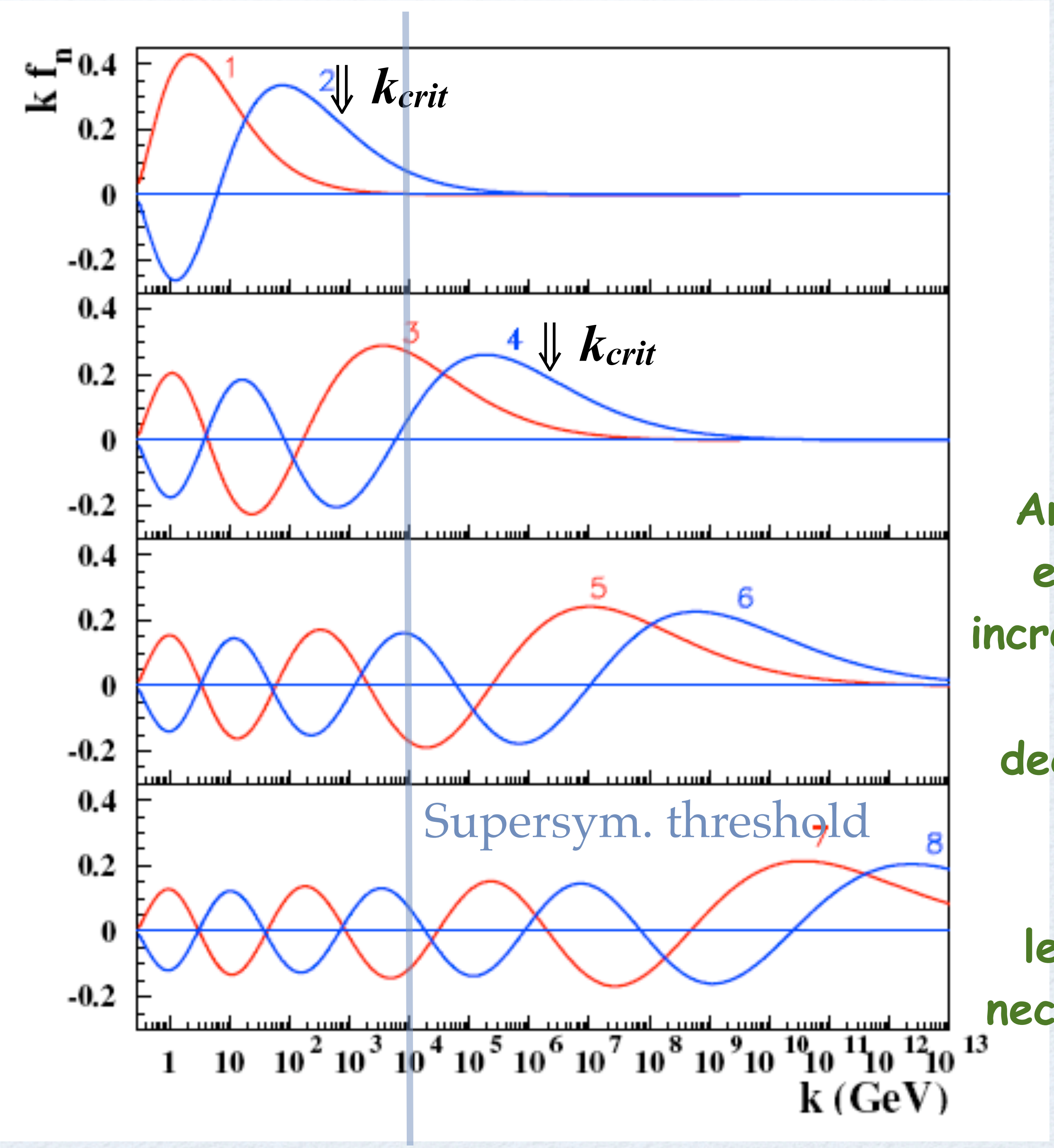

Are BSM effects increasing ν ? and decreasing k_{crit} ?

less ef's necessary ?

Transition to the saturation and confinement regions

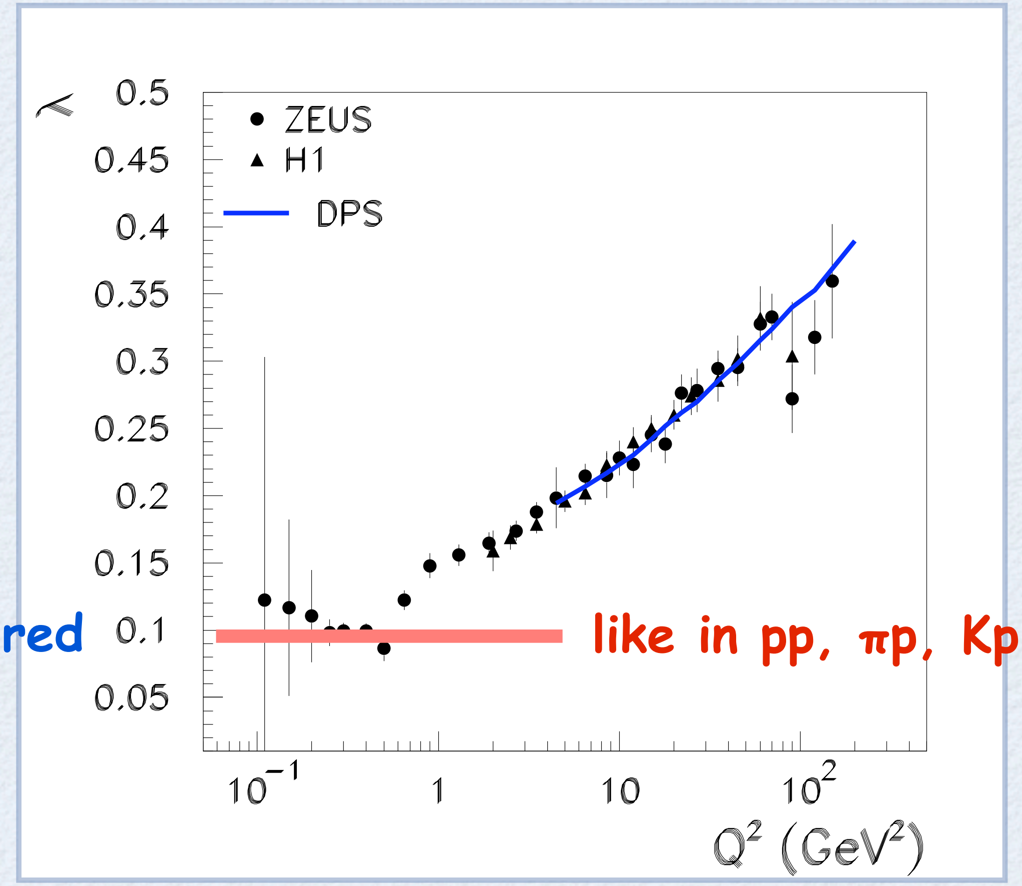

precision data
at low Q^2 required

like in pp, πp, Kp scattering

evaluate triple pomeron vertex with DPS, at $t \neq 0$, apply it in the saturation region, i.e at low Q^2 , and to elastic pp scattering

High energy behaviour of $pp, \pi p, Kp$ and γp shows universal properties ☞ get insight into confinement?

Pomeron-Graviton Correspondence

String theory emerged out of
phenomenology of hadron-hadron scattering

Dolan-Horn-Schmid duality between
s-channel and t-channel Regge-pole description
of hadronic X-sections

$$\sum_r \frac{g_r^2(t)}{s-(M_r-i\Gamma_r)^2} \simeq \beta(t)(-\alpha' s)^{\alpha(t)} \, .$$

➔ Veneziano amplitude

$$A_{\pi^+\pi^-\to\pi^+\pi^-}(s,t) = g_o^2 \, \frac{\Gamma[1-\alpha_\rho(t)]\Gamma[1-\alpha_\rho(s)]}{\Gamma[1-\alpha_\rho(s)-\alpha_\rho(t)]}$$

generalization of V-amplitude ➔ dual models
➔ mesons are open strings
L - string length, $E = c\,L$, $J = \alpha' E^2$

$\alpha(t) = \alpha_0 + \alpha' t$

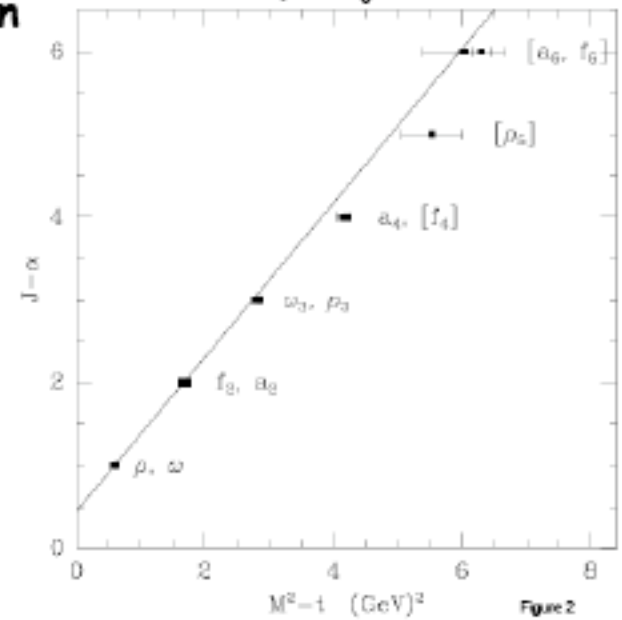

Figure 2

V-amplitude for $\alpha(0) = 1$ has a pole at $s = t = 0$
with $J = 2$, a graviton ➔ starting point for theory of quantum gravity

Superstring Theory, Green, Schwarz, Witten (1987)
R. Brower hep-th/0508036

Maldacena Conjecture

from the talk by J. Maldacena

Particle theory = gravity theory

Most supersymmetry QCD theory	=	String theory on $AdS_5 \times S^5$	(J.M.)

N colors

N = magnetic flux through S^5

Radius of curvature $$R_{S^5} = R_{AdS_5} = \left(g_{YM}^2\ N\right)^{1/4} l_s$$

Duality:

$g^2 N$ is small → perturbation theory is easy – gravity is bad

$g^2 N$ is large → gravity is good – perturbation theory is hard

Strings made with gluons become fundamental strings.

Pomeron and Gauge/String Duality

Brower, Polchinski, Strassler, and Tan, hep-th/0603115

Pomeron is a coherent color-singlet object, build from gluons, with universal properties; it is the object which is exchanged by any pair of hadrons that scatter at high energies.

$$j^0 = 2 - \frac{2}{\pi\sqrt{\bar{\alpha}_s}}$$

in ADS$_5$ and in N=4 Super YM

Kotikov, Lipatov, Onishchenko, Velizhanin, Physt. Lett. B 632, 754 (2006)

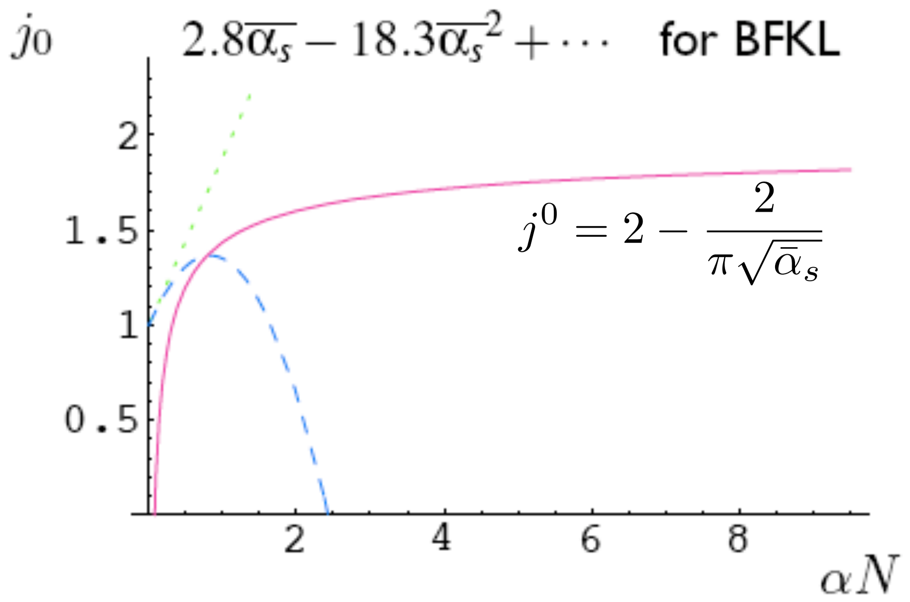

$$\left(\overline{\alpha_s} = \frac{\alpha_s N_C}{\pi}\right)$$

The String "Pomeron" in Flat Space

Doug Ross

Pomeron amplitude can be obtained from exchange of closed string between states with wavefunctions

$$\Psi_1(x_1),\ \Psi_2(x_2), \Psi_3(x_3), \Psi_4(x_4)$$

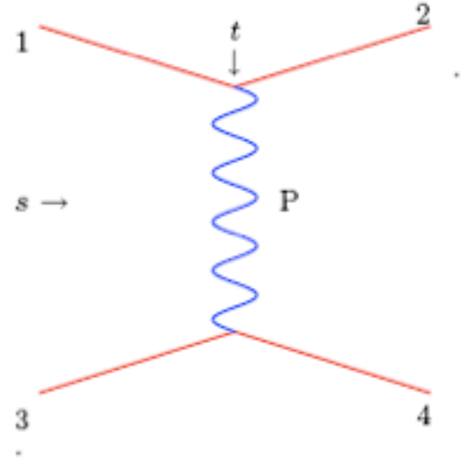

In flat space

$$\Psi_i(x) = e^{ip_i\cdot x}, \quad x^\mu,\ (\mu = 0\cdots 9)$$

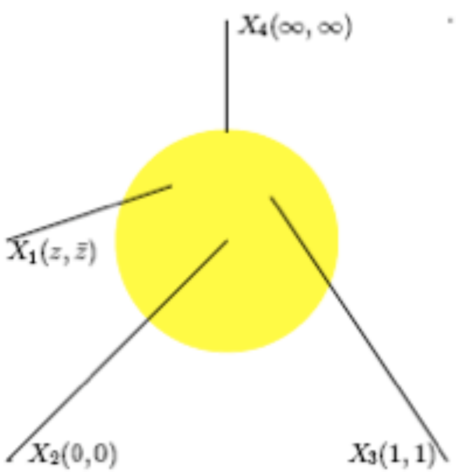

$$\mathcal{A}(s,t) \sim \int D[X] e^{i\int dz d\bar{z} \mathcal{L}_{string}[X(z,\bar{z})]}$$

$$\times \Psi_1(X(z,\bar{z})\Psi_2(X(0,0)\Psi_3(X(1,1)\Psi_4(X(\infty,\infty))$$

$$\sim \quad s^{2+\frac{1}{2}\alpha' t}$$ (Regge Limit: $s \gg t \gg 1/\alpha'$)

Extension to Curved Space

Doug Ross

$$s^{2+\frac{1}{2}\alpha' t} = \Psi_1^*(x)\Psi_2^*(x) s^{2+\frac{1}{2}\alpha' \nabla^2} \Psi_1(x)\Psi_2(x)$$

Exponent 2 since t=0 state is a graviton, (j=2)

$u = \ln(r/r_0)$ $\qquad\qquad$ $AdS \times S^5$

$$ds^2 = \frac{e^{2u}}{R^2}\eta_{\mu\nu}dx^\mu dx^\nu + R^2 du^2 - \sum_{M,N=1}^{5} g_{MN} dy^M dy^N$$

In N=4, SUSY YM, $R^2 = \alpha'(g_{YM}^2 N_c)$

S^5 is very compact - Only consider zero energy modes on this space.

In this space ∇^2 must be replaced by Laplacian in curved space

In curved space ∇^2 depends on spin of particle on which it acts.
We take j=2, since trajectory corresponds to graviton at $t = 0$

$$\nabla^2_{AdS} = R^2 e^{-2u} \nabla^2_{(4)} + \frac{1}{R^2}\left(\partial_u^2 - 4\right)$$

Acting on $\Psi_1(x)\Psi_2(x)$ we can write this as

$$\nabla^2_{AdS} = R^2 e^{-2u} t + \frac{1}{R^2}\left(\partial_u^2 - 4\right)$$

$$\mathcal{A}(s,t,u_1,u_2) \sim \phi_3(u_1)\phi_4(u_1)s^{2+\frac{1}{2}\alpha'\left[R^2e^{-2u}t+(\partial_u^2-4)/R^2\right]}\phi_2(u_2)\phi_1(u_2)$$

This is solved by finding the eigenfunctions

Doug Ross

$$\phi_\nu(u)$$

and eigenvalues

$$\chi(\nu)$$

of the operator

$$\nabla^2_{AdS} = R^2e^{-2u}t + \frac{1}{R^2}\left(\partial_u^2 - 4\right)$$

$$\mathcal{A}(s,t,u_1,u_2) \sim \int d\nu\, s^{2+\frac{1}{2}\alpha'\chi(\nu)}\phi_\nu^*(u_1)\phi_\nu(u_2)$$

For t=0: $\phi_\nu(u) = e^{i\nu u}, \quad \chi = -\frac{(4+\nu^2)}{R^2}$

$$\mathcal{A}(s,t,u_1,u_2) \sim \int d\nu\, s^{2-\alpha'(2/R^2-\nu^2/(2R^2)}e^{i\nu(u_1-u_2)}$$

Similarity with BFKL

BPST - Diffusion in ADS_5

String result

$$\mathcal{A}(s,t,u_1,u_2) \sim \int d\nu\, s^{2-\alpha'(2/R^2-\nu^2/(2R^2))} e^{i\nu(u_1-u_2)}$$

BFKL result

$$\mathcal{A}(s,t,\mathbf{k_1},\mathbf{k_2}) \sim \int d\nu\, s^{1+\overline{\alpha_s}(4\ln(2)-7\zeta(3)\nu^2+\cdots)} e^{i\nu(ln(\mathbf{k_2})-ln(\mathbf{k_1}))}$$

⇒ ln(k) can be identified with u

Brower, Polchinski, Strassler, and Tan, hep-th/0603115

$$j_0 = 1 + \frac{4\ln 2}{\pi}\alpha N\ , \quad \mathcal{D} = \frac{7\zeta(3)}{2\pi}\alpha N\ .$$

$$\mathcal{K}(p_\perp, p'_\perp, s) \approx \frac{s^{j_0}}{\sqrt{4\pi\mathcal{D}\ln s}} e^{-(\ln p'_\perp - \ln p_\perp)^2/4\mathcal{D}\ln s}$$

BPST- similarity of diffusion in BFKL-k, position-space-x_T and ADS_5-u variables

$$\int d^{d-2}k_\perp e^{i\mathbf{k}_\perp\cdot\mathbf{x}_\perp} s^{\alpha(t)} \approx s^{\alpha_0} \int d^{d-2}k_\perp e^{i\mathbf{k}_\perp\cdot\mathbf{x}_\perp} e^{-\alpha' k_\perp^2 \ln s} = \frac{s^{\alpha_0} e^{-x_\perp^2/4\alpha'\ln s}}{(4\pi\alpha'\ln s)^{(d-2)/2}}\ .$$

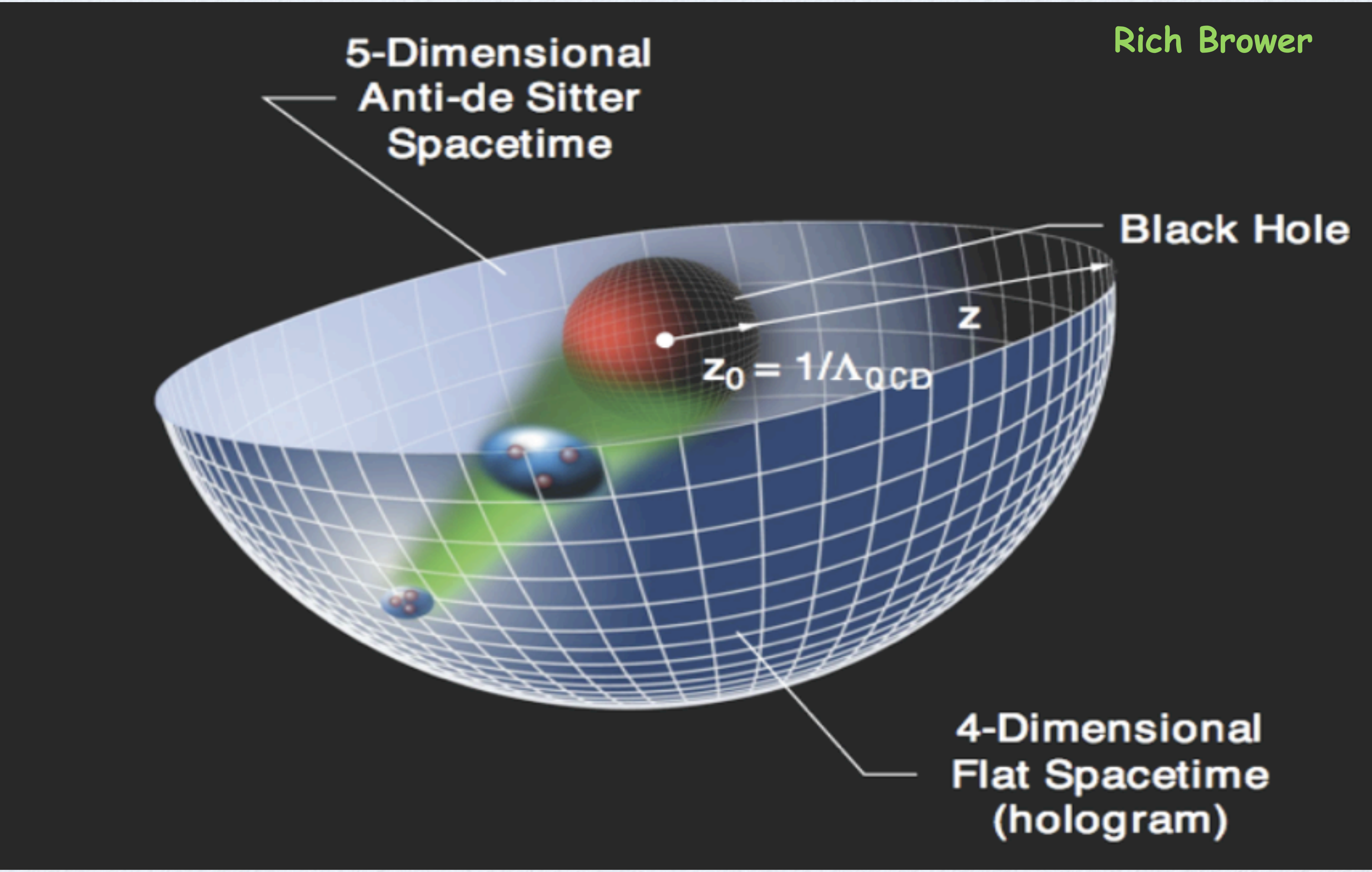

$u = \ln(z_0/z)$ $\qquad$ $u = \ln k$

Introducing Confinement effects in Infrared Region

Model dependent

Hard-wall model

Doug Ross

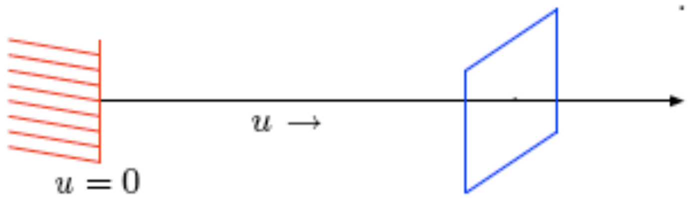

Need eigenvalues of ∇^2_{AdS} but with boundary conditions near $u = 0$

$$\phi_u \sim e^{2u} \sim 1 + 2u$$

For $t = 0$ eigenfunctions are

$$\phi_\nu(u) = e^{-i\nu u} + R_0(\nu) e^{+i\nu u}$$

$$R_0(\nu) = \frac{1 + \frac{i}{2}\nu}{1 - \frac{i}{2}\nu}$$

so that $\phi_\nu(u) \sim 1 + 2u$ near $u = 0$.

eigenfunctions are composed of plain and reflected wave

BPST:

for t>0 the hard wall model leads to glueballs, which are the discrete spectrum of 'cavity modes' of the Laplacian for a five-dimensional spin-two field

Running Coupling

If g_{YM} runs with u, with negative β-function, then to leading order

$$R^2 = \sqrt{\frac{4\pi\alpha'}{\beta_0 u}}$$

Change of variable from u to w, where

$$u = Cw^{\frac{4}{3}}$$

$$ds^2 = e^{2Cw^{4/3}}\eta_{\mu\nu}dx^\mu dx^\nu + \alpha' dw^2$$

Eigenvalue equation:

$$\frac{\partial^2}{\partial w^2}\phi_j(w) = \left(\left(\frac{8}{3}C\right)^2 w^{2/3} - t\,e^{-2Cw^{4/3}} + 2(j-2)\right)\phi_j(w)$$

$$\frac{\partial^2}{\partial w^2}\phi_j(w) = \left(\left(\frac{8}{3}C\right)^2 w^{2/3} - t\,e^{-2Cw^{4/3}} + 2(j-2)\right)\phi_j(w)$$

For $t < 0$ effective potential has a minimum - it grows as $w \to 0$ and as $w \to \infty$

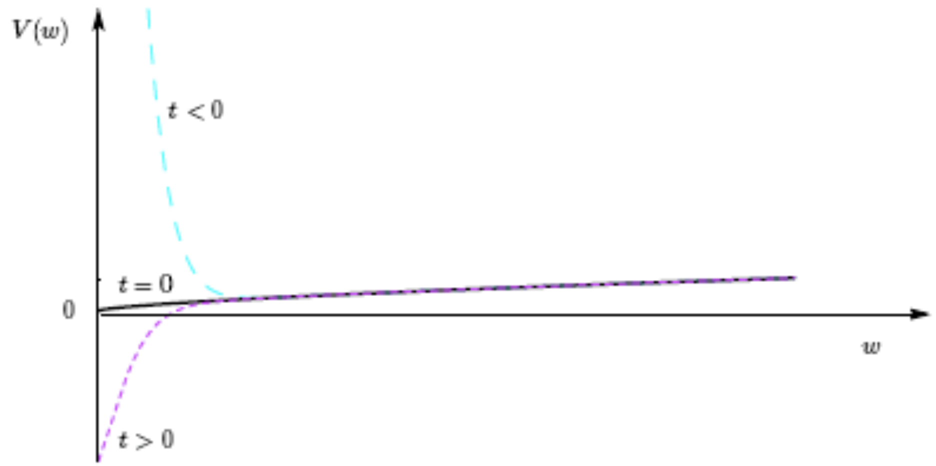

Potential well - discrete values of j

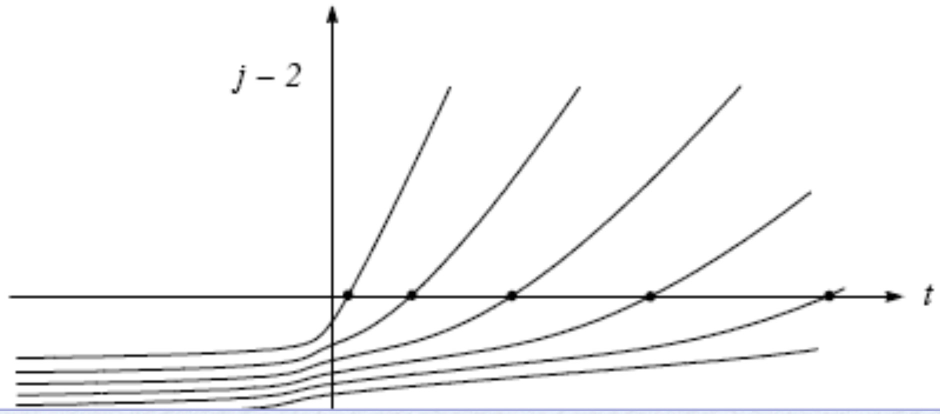

String-Gauge Dual Description of Deep Inelastic Scattering at Small-x

arXiv: 1007.2259v2, Sept 2010

Richard C. Brower[*], Marko Djurić[†], Ina Sarčević[‡§] and Chung-I Tan[¶]

direct term

reflected term

$$F_2(x,Q^2) = \frac{g_0^2 \rho^{3/2}}{32\pi^{5/2}} \int dz dz' P_{13}(z,Q^2) P_{24}(z')(zz'Q^2)\, e^{(1-\rho)\tau} \left(\frac{e^{-\frac{\log^2 z/z'}{\rho\tau}}}{\tau^{1/2}} + \mathcal{F}(z,z',\tau) \frac{e^{-\frac{\log^2 zz'/z_0^2}{\rho\tau}}}{\tau^{1/2}} \right)$$

reflected term (model dependent) corresponds to the phase condition in KLRW

$$P_{13}(z) \approx C\delta(z - 1/Q).$$

$$P_{24}(z') \approx \delta(z' - 1/Q').$$

$$e^{(1-\rho)\tau} \sim (1/x)^{1-\rho}$$

$$\mathcal{F}(z,z',\tau) = 1 - 2\sqrt{\rho\pi\tau}\, e^{\eta^2} erfc(\eta), \qquad \eta = \frac{-\log \frac{zz'}{z_0^2} + \rho\tau}{\sqrt{\rho\tau}}.$$

fitted variables,

g_0, ρ, z_0, Q'

in KLRW, ρ is predicted

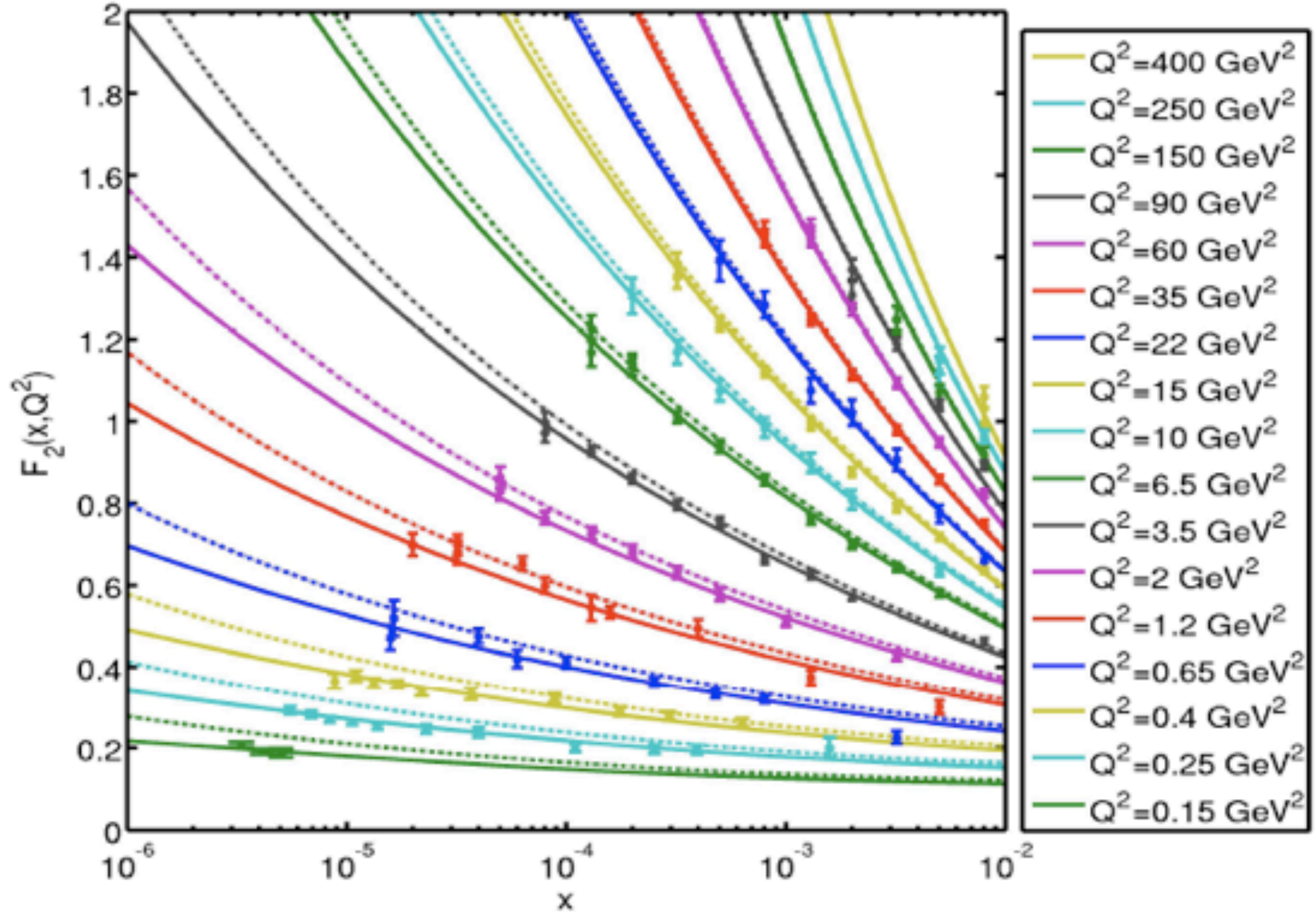

Figure 9: Fit to the combined H1-ZEUS small-x data for $F_2(x, Q^2)$ by a hard-wall eikonal treatment. We have exhibited both the hard-wall single Pomeron fits, (in dashed lines), and the hard-wall eikonal, (in solid lines), together for a better visual comparison. The fit include 249 data points, with $x < 10^{-2}$, and 34 Q^2 values, ranging from 0.1 GeV^2 to 400 GeV^2. Only data set for 17 Q^2 values are shown.

Summary and Outlook

Since the beginning of particle physics, high energy behavior of scattering amplitudes was expected to give basic insight into the nature of strong forces. (at HE, time dilatation slows down the dynamics of physical processes)

Two different basic approaches: the Discrete-BFKL-Pomeron and ADS-closed-string-Pomeron are describing HERA F_2 data very well.

Will striking similarities between the two approaches give insight into the connection between QCD and Gravitation? Into the confinement problem?

Precise measurement at future ep and eA could provide crucial data:

1) exclusive diffractive processes $\Rightarrow$ measurements of $\alpha(t)$ - EIC

2) F_2 and exclusive diffraction at highest possible energies - LHeC

Summary and Outlook

High energy behavior of scattering amplitudes was always considered to

expected to give basic insight into the nature of strong forces
Two different basic approaches to the pomeron problem
Discrete Pomeron Solution of the BFKL eq. and ADS-Pomeron are describing HERA F_2 data very well

Can we tell something about the gluon-gluon interaction
in the confinement region?
in the BSM region?

Outlook:
Formulate DPS at $t \neq 0$, apply it to diffractive processes

evaluate triple pomeron vertex with DPS, apply it in the saturation region, i.e at low Q^2 , and to elastic pp scattering

Back up slides

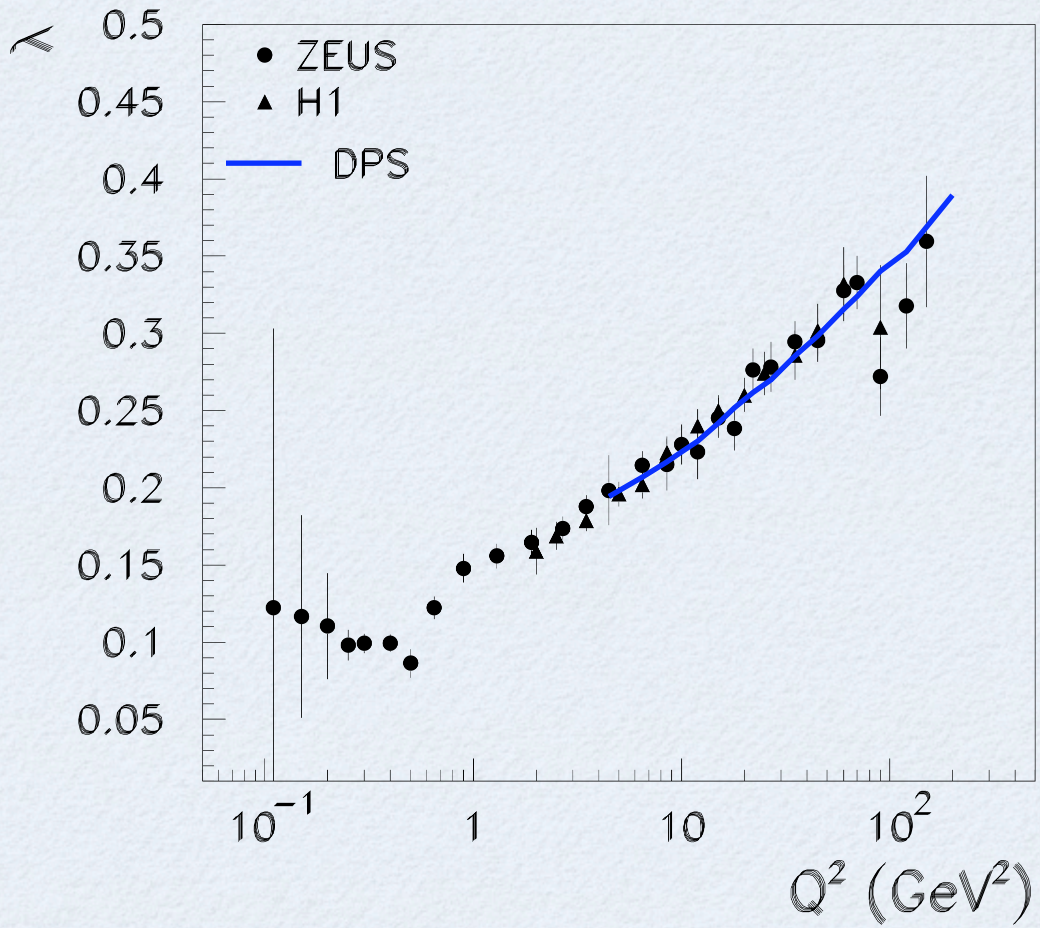

ZEUS
H1
DPS
λ
0.5
0.45
0.4
0.35
0.3
0.25
0.2
0.15
0.1
0.05
10^{-1}
1
10
10^2
Q^2 (GeV^2)

Quasi-locality of the kernel

$$\mathcal{K}(\mathbf{k}, \mathbf{k}') = \frac{1}{kk'} \sum_{n=0}^{\infty} c_n \delta^{(n)} \left(\ln(\mathbf{k}^2/\mathbf{k}'^2) \right) ,$$

and of the Green function

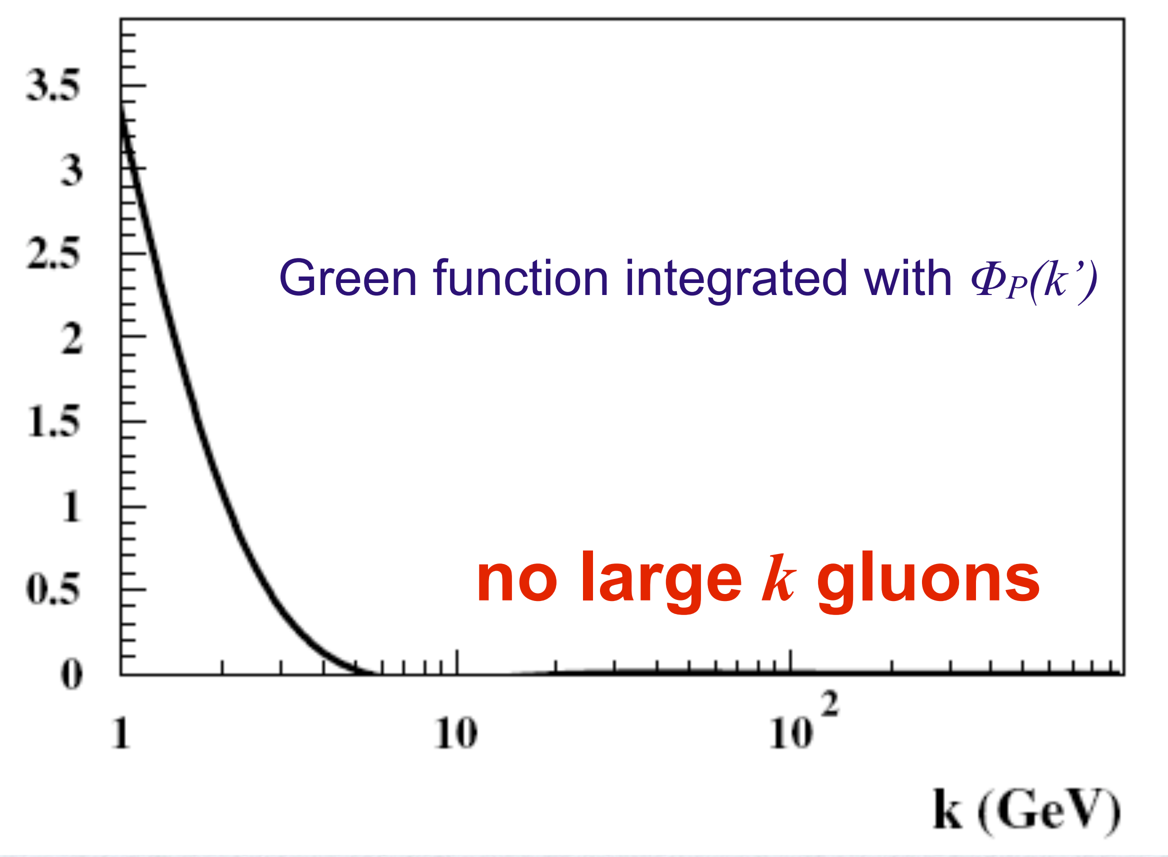

$$k \int dk'^{\,2} \mathcal{K}(\mathbf{k},\mathbf{k}') f_\omega(\mathbf{k}') \;=\; \chi\left(-i\frac{d}{d\ln k^2}, \alpha_s(k^2)\right)\bar{f}_\omega(k) \;=\; \omega \bar{f}_\omega(k)$$

semiclassical approximation

$$\left(\frac{d}{d\ln(k)}\right)^r \bar{f}_\omega(k) \;\approx\; \bar{f}_\omega(k)\left(\frac{d\ln \bar{f}_\omega(k)}{d\ln k}\right)^r$$

$$\chi\left(-i\frac{d\ln \bar{f}_\omega(k)}{d\ln k^2}, \alpha_s(k^2)\right) \;=\; \omega$$

$$\frac{d\bar{f}_\omega(k)}{d\ln(k^2)} \;=\; i\nu_\omega(\alpha_s(k^2))\bar{f}_\omega(k)$$

DGLAP

semiclassical approximation

$$\left| \frac{d}{d \ln k} \ln\left(\nu(\mathbf{k})\right) \right| \ll \nu(\mathbf{k})$$

$$f_\omega(\mathbf{k}) = \frac{C(\nu(\mathbf{k}))}{k} \exp\left(2i \int^{\ln(k)} \nu(\mathbf{k}') d\ln k' \right)$$

σ_L/σ_T

KMW

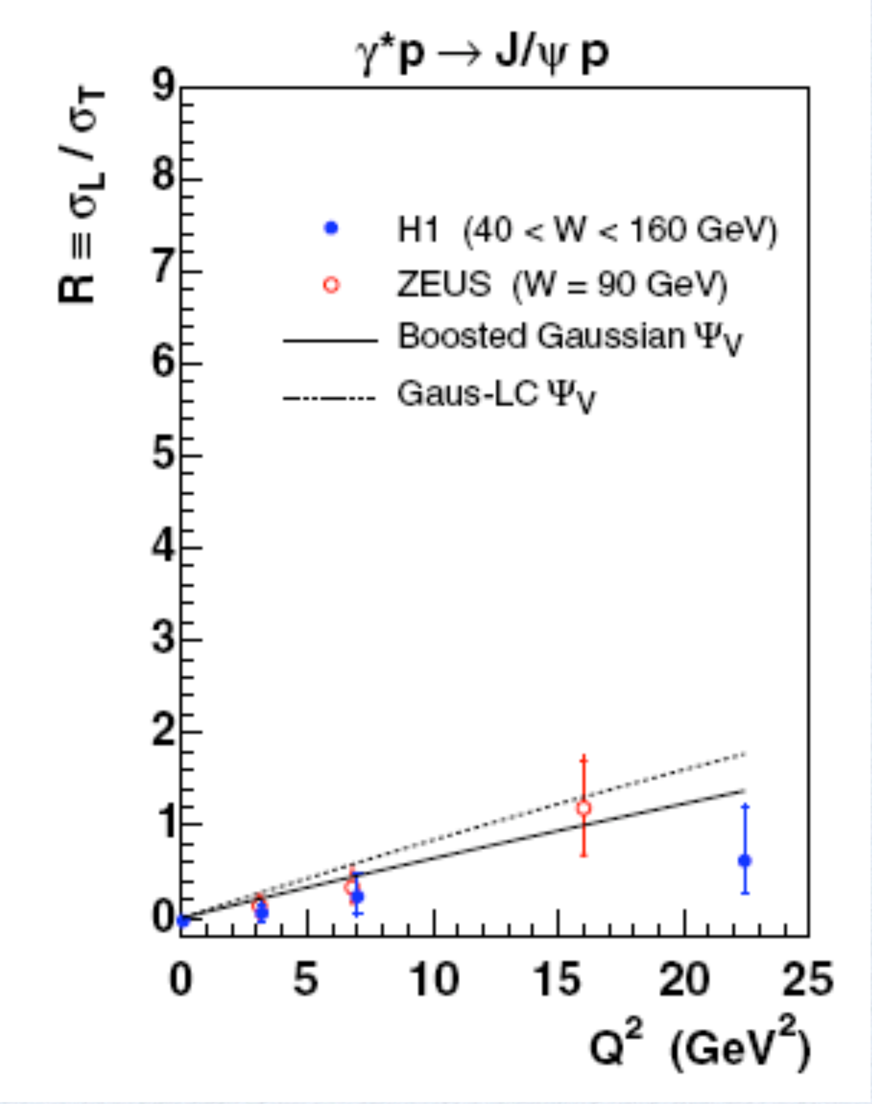

DVCS

KMW

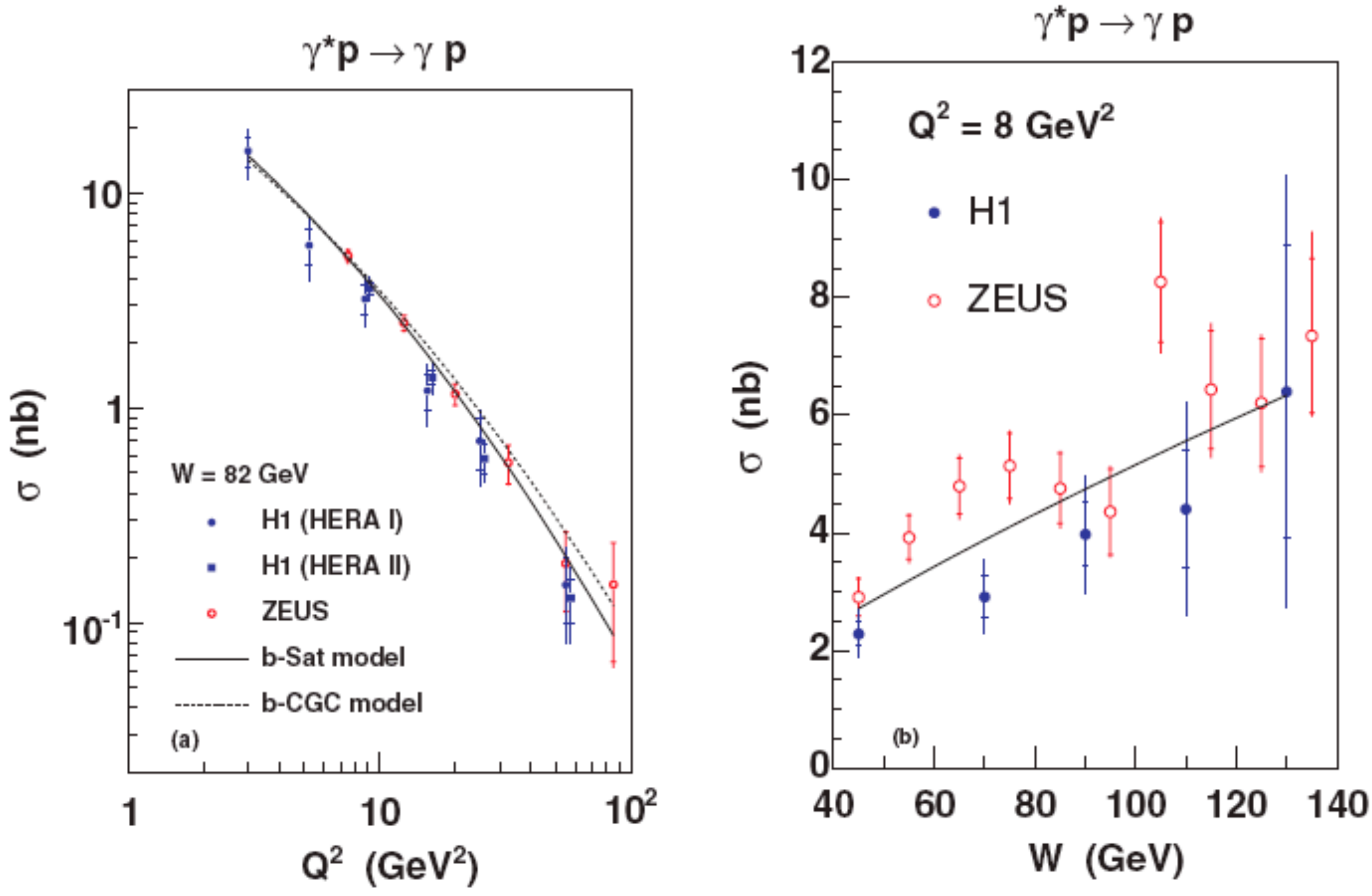

γ*p → γ p
σ (nb)
10
1
10^-1
W = 82 GeV
H1 (HERA I)
H1 (HERA II)
ZEUS
b-Sat model
b-CGC model
(a)
1
10
10^2
Q^2 (GeV^2)
γ*p → γ p
Q^2 = 8 GeV^2
H1
ZEUS
σ (nb)
0
2
4
6
8
10
12
(b)
40
60
80
100
120
140
W (GeV)

Partons vs Dipoles

Infinite momentum frame: Partons

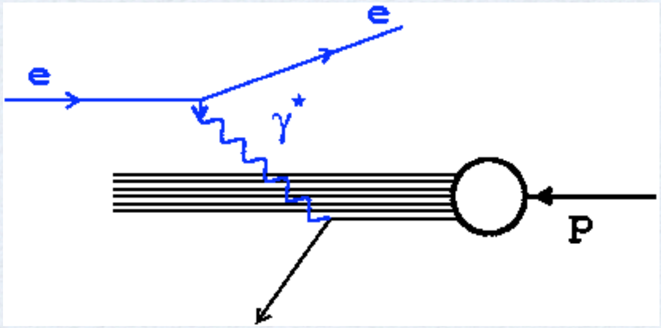

F_2 measures parton density at a scale Q^2

$$F_2 = \frac{Q^2}{4\pi^2 \alpha_{em}} \sigma_{tot}^{\gamma^* p} = \Sigma_f e_f^2 x q(x, Q^2)$$

Proton rest frame: Dipoles - long living quark pair interacts with the gluons of the proton *dipole life time ≈ 1/(m_p x)*

= 10 - 1000 fm at x = 10^{-2} - 10^{-4}

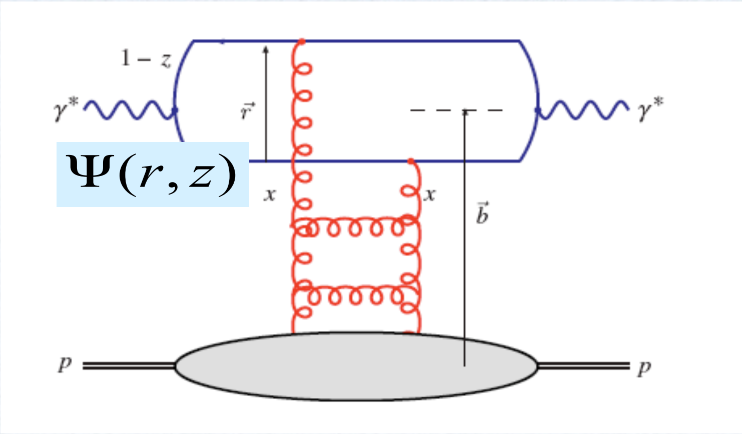

$$\sigma_{tot}^{\gamma^* p} = \int \Psi(z, r^2)^* \sigma_{qq} \Psi(z, r^2)$$

for small dipoles, at low-x, dipole picture is equivalent to the QCD parton picture

$$\sigma_{qq} \propto x\, g(x, \mu^2)$$

Combining ZEUS and H1 F_2 data

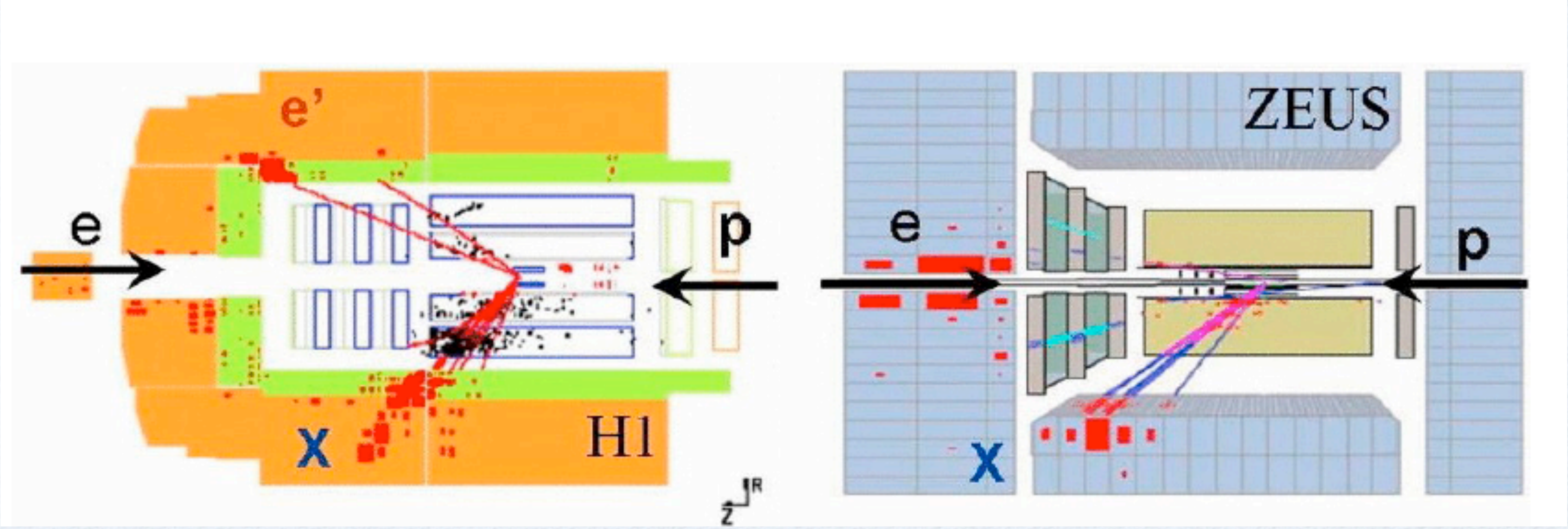

H1 and ZEUS collected similar amount of data: 100 pb^{-1}

➥ improved statistical precision by ~ $1/\sqrt{2}$

Improved systematic precision

H1 and ZEUS detectors and data analysis are quite different.

➥ The H1 and ZEUS cross-sections have different sensitivities to similar sources of correlated systematic uncertainties